

NASA TM SX-242

Library Copy
RA-C322117UN 12/31/71
CCN-215-2

C1

DECLASSIFY BY ~~10~~
CCN-215-2

TECHNICAL MEMORANDUM

SX-242

IN-08
280 419
DATE 10/1/71

for the

Office of Naval Research

TRANSONIC FLUTTER INVESTIGATION OF MODELS OF T-TAIL OF BLACKBURN NA-39 AIRPLANE

By George W. Jones, Jr., and Moses G. Farmer

Langley Research Center
Langley Field, Va.LIBRARY COPY **B**

DEC 11 1959

LANGLEY RESEARCH CENTER
LIBRARY, NASA
LANGLEY FIELD, VIRGINIA

CLASSIFIED DOCUMENT - TITLE UNCLASSIFIED

This material contains information affecting the national defense of the United States within the meaning of the espionage laws, Title 18, U.S.C., Secs. 793 and 794, the transmission or revelation of which in any manner to an unauthorized person is prohibited by law.

NATIONAL AERONAUTICS AND SPACE ADMINISTRATION
WASHINGTON

DEC 9 1959


NATIONAL AERONAUTICS AND SPACE ADMINISTRATION

TECHNICAL MEMORANDUM SX-242

for the

Office of Naval Research

TRANSONIC FLUTTER INVESTIGATION OF MODELS OF T-TAIL
OF BLACKBURN NA-39 AIRPLANE*

By George W. Jones, Jr., and Moses G. Farmer


SUMMARY


A transonic flutter investigation has been made of models of the T-tail of the Blackburn NA-39 airplane. The models were dynamically and elastically scaled from measured airplane data in accordance with criteria which include a flutter safety margin. The investigation was made in the Langley transonic blowdown tunnel and covered a Mach number range from 0.73 to 1.09 at simulated altitudes extending to below sea level.

The results of the investigation indicated that, if differences between the measured model and scaled airplane properties are disregarded, the airplane with the normal value of stabilizer pitching stiffness should have a stiffness margin of safety of at least 32 percent at all Mach numbers and altitudes within the flight boundary. However, the airplane with the emergency value of stabilizer pitching stiffness would not have the required margin of safety from symmetrical flutter at Mach numbers greater than about 0.85 at low altitudes.

First-order corrections for some differences between the measured model and scaled airplane properties indicated that the airplane with the normal value of stabilizer pitching stiffness would still have an adequate margin of safety from flutter and that the flutter safety margin for the airplane with the emergency value of stabilizer pitching stiffness would be changed from inadequate to adequate. However, the validity of the corrections is questionable.

* Title, Unclassified.






INTRODUCTION

A preliminary transonic flutter investigation of the models of the T-tail of the Blackburn NA-39 airplane was reported in reference 1. The investigation was made in the Langley transonic blowdown tunnel and was undertaken at the request of the Office of Naval Research. The results indicated that if the models simulated the airplane in all important respects, the airplane tail would have at least the required 32-percent stiffness margin of safety from flutter at sea level at Mach numbers up to 0.9. At Mach numbers between 0.9 and 1.0 antisymmetric flutter and symmetric oscillations of the stabilizer which may have been symmetric flutter were both obtained; however, the data were insufficient to establish whether the margin of safety was adequate at sea level at Mach numbers above 0.9. Since the models used in the investigation were scaled using estimated airplane properties, the results were considered tentative pending confirmation of the airplane properties.

After the preliminary investigation of reference 1, measurements of the airplane T-tail physical properties were made by Blackburn and General Aircraft, Ltd. and these data were supplied to the National Aeronautics and Space Administration. Examination of the measured airplane properties indicated that the models of reference 1 did not adequately simulate the airplane. Therefore, a second transonic flutter investigation has been made using models scaled from the measured airplane properties and the results of the second investigation are reported herein.

The T-tail of the airplane consists of an all-movable sweptback stabilizer mounted on top of a sweptback fin. The incidence of the stabilizer is controlled by two hydraulic actuators which rotate the surface about an axis located at 52 percent of the center-line chord of the stabilizer. However, the airplane is required to be free from flutter in an emergency condition in which only one actuator is operable. The stabilizer pitching stiffness with two actuators operable is denoted herein as the normal pitching stiffness and the stiffness with one actuator operable is denoted as the emergency pitching stiffness. The stabilizer is equipped with a two-position trailing-edge elevator which is locked in the plane of the stabilizer surface at high speeds and can be moved to a fixed deflection angle at low speeds. The fin is equipped with an unbalanced trailing-edge rudder which is actuated from an attachment at the root. It is not planned to use viscous dampers on any of the T-tail components of the NA-39 airplane.

Three different types of flutter of the T-tail have appeared possible: antisymmetric flutter of the T-tail unit as a whole with little or no control-surface motion, symmetric flutter of the all-movable horizontal tail, and flutter or buzz of the rudder. Flutter involving elevator



motion was considered unlikely because elevator frequencies in the locked position are very high compared with the fundamental frequencies of the surfaces. Accordingly, the models of both the preliminary and present investigations were provided with rudders but the elevators were made integral with the stabilizers.

In the present investigation the models were mounted at approximately zero angle of attack on a sting mount which provided flexibility in the fuselage vertical bending, side bending, and torsion degrees of freedom. The physical properties of the models of the present investigation differed from those of reference 1 chiefly as follows: The rudder rotation stiffness and frequency were reduced considerably, the stabilizer fundamental bending frequency was increased, a fuselage vertical bending degree of freedom was added, and the fuselage side bending frequency was increased considerably.

SYMBOLS

b	local streamwise semichord of fin or stabilizer, ft
c	local streamwise chord of stabilizer, ft
l	length scale factor, $\frac{\text{Typical model length}}{\text{Corresponding airplane length}}$
M	Mach number
m	mass scale factor, $\frac{\text{Typical model mass}}{\text{Corresponding airplane mass}}$
m'	mass of stabilizer, slugs
q	dynamic pressure, lb/sq ft
s	value of y at stabilizer tip, ft
T	static temperature, °R
t	time scale factor, $\frac{\text{Time required for tunnel airstream to move 1 model chord length}}{\text{Time required for airplane to move 1 airplane chord length}}$
V	velocity, ft/sec

\bar{V} reduced velocity based on a representative natural frequency,

$$\frac{V}{b\omega_1}$$

$$v = \frac{\pi}{4} \int_{-s}^s c^2 dy, \text{ cu ft}$$

y distance along stabilizer from stabilizer center line, measured perpendicular to stabilizer center line, ft

λ stiffness reduction factor used to provide margin of safety in application of model flutter test results to airplane

μ mass ratio, $\frac{m'}{\rho v}$

ρ static air density, slugs/cu ft

ω_1 representative natural frequency, radians/sec

Subscripts:

A airplane

M model

MODELS

Geometry

For this investigation, two models of the T-tail of the Blackburn NA-39 attack airplane were used. These models, which are designated model 5 and model 6, are scaled geometrically to 1/12 airplane size. A photograph of the model is shown in figure 1 and a sketch of the model is shown in figure 2. Some of the more important geometric properties are given in table I. Although models 5 and 6 have the same external geometry, their physical properties differ as will be discussed under the section entitled "Physical Properties."

The stabilizer had an aspect ratio of 2.64, a taper ratio of 0.582, and a thickness-chord ratio of 0.05 based on the streamwise chord. The stabilizer leading and trailing edges were swept back 29° and 9° , respectively. The stabilizer pitch axis was located at the 52-percent station of the center-line chord. Although the stabilizer sections on the

airplane are cambered, the stabilizer sections on the models are not cambered. From past experience, the use of models without camber is not thought to affect the flutter results and is preferred because the model usually can be trimmed more easily in the tunnel.

On the airplane the leading edge of the fin is curved and extends forward to the canopy to form a long dorsal fin. On the models the lower part of the fin leading edge was arbitrarily curved downward and terminated as indicated in figures 1 and 2. The maximum thickness of the fin-rudder varied from 11 percent of the local streamwise chord at the root to 8 percent at the minimum chord (fig. 2). The leading edge of the main spar of the fin was swept back 27° . The fin-rudder trailing edge and the rudder hinge line were swept back 22° . The rudder chord was constant and was 30.4 percent of the minimum fin-rudder chord.

Scaling

In scaling the airplane properties, the nondimensional mass and stiffness distributions were required to be the same for the models as for the airplane. The mass and stiffness levels for the models were obtained by specifying the scale factors for the fundamental quantities involved: length, mass, and time.

The size of the model was limited by tunnel-wall-interference effects, and on the basis of past experience the length scale factor was chosen to be

$$l = \frac{1}{12} \quad (1)$$

The mass scale factor was obtained from the requirement that the mass ratio μ should be the same for the model as for the airplane, which results in

$$m = \frac{\rho_M}{\rho_A} l^3 \quad (2)$$

In order to locate the simulated sea-level altitude near the middle of the tunnel density range available at a Mach number of 1.00, the

density ratio was chosen to be $\frac{\rho_M}{\rho_A} = 1.97$. This location of simulated sea level allows altitudes below sea level to be obtained and flutter margins to be indicated where flutter does not occur above sea level.

The time scale factor was obtained from the requirement that the reduced velocity \bar{V} should be the same for the model as for the airplane, which results in

$$t = \left(\frac{V_M}{V_A} \right)^{-1} l$$

Since the Mach number is the same for the model as for the airplane, the time scale factor may be written

$$t = \left(\frac{T_M}{T_A} \right)^{-1/2} l \quad (3)$$

The static temperature for the airplane T_A is a function only of altitude, and for sea-level altitude it was taken to be 519°R . However, in the tunnel during a run, the temperature continually drops as air is expended from the reservoir and the temperatures obtained at the various flutter points during an investigation are different. A study of previous flutter data indicated that 408°R was near the average value of the static temperature that would be expected during the present investigation, and this assumed value was used to obtain the temperature ratio

used in the scaling: $\frac{T_M}{T_A} = 0.786$.

A list of the pertinent model and flow quantities and the design scale factors used is given in table II. It may be noted that the factor λ is used in the scale factors for some of the quantities listed in table II. The factor λ has the value of 0.76 and occurs because the model stiffnesses were made 76 percent of those which would result from application of the scale factors as specified (eqs. (1) to (3)). The reduced model stiffnesses provided a margin of safety in the application of the model flutter test results to the airplane. Thus, the design reduced velocity for the model is equal, not to that of the airplane, but to that of an airplane having stiffnesses 76 percent of those of the actual airplane.

The dynamic pressure and Mach number are quantities which are controllable during a run, whereas the temperature is not. If the dynamic pressure and Mach number are considered to be fixed and a static temperature different from the design value is obtained, both the density and velocity will be different from the values considered in the scaling. The density and velocity changes result, respectively, in values of mass ratio and reduced velocity different from the design values. However,

a combination of reduced velocity and mass ratio which can be expressed in terms of the dynamic pressure

$$\frac{\bar{V}_M^2}{\mu_M} \propto q_M$$

is independent of the temperature, and this combination is exactly simulated in the runs by the expedient of interpreting the simulated altitude in terms of dynamic pressure. Thus, the scale factor in table II for dynamic pressure is used to convert the dynamic pressure for the airplane at any altitude and Mach number to the dynamic pressure for the model at the same altitude and Mach number. The dynamic pressure for the airplane is assumed to be that calculated by use of the ICAO standard atmosphere (ref. 2). It may be noted that for a given altitude q/M^2 is a constant.

The effect of not satisfying exactly the individual values of mass ratio and reduced velocity is believed to be negligible in the present investigation. Experience with a wide variety of flutter models has indicated that, at least within the operational limits of the tunnel, flutter at a given Mach number tends to occur at a constant value of dynamic pressure regardless of the individual values of density and velocity.

Construction

Some of the construction details of the models are indicated in the X-ray photographs of figure 3. The main fin spar (figs. 3(a) and 3(c)) was constructed by welding together four hollow beams with trapezoidal cross sections which had been fabricated from aluminum-alloy sheet. The main stabilizer spar (figs. 3(b) and 3(d)) consisted of three beams of a similar type of construction. This construction resulted in wide main spars which simulated the multispar arrangement used in the airplane. In the model stabilizer and fin, aluminum ribs were welded to the main spar. The leading and trailing edges were pine. Balsa was used to fill the surfaces to contour. Lead weights were placed in the stabilizer and rudder at various locations in order to obtain the desired mass distribution. Slits were cut in the fin spar to lower the stiffness. The rudder was constructed with an aluminum-alloy leading edge and ribs, pine trailing edge, and balsa filler. The various surfaces were wrapped with silk cloth and lacquered. Strain gages were installed on the main fin spar near the fin root and on the stabilizer pitch axis near the fin-stabilizer juncture.

The stabilizer was attached to the fin by a T-shaped fitting at the pitch-axis location and by a U-shaped spring fitting farther forward

(fig. 3). The U-shaped spring mounting position was reversed on models 5 and 6 as may be seen in figures 3(a) and 3(c). Adjustments in the dimensions and location of the U-shaped fitting provided the desired stiffness between the stabilizer and the fin in the stabilizer pitching degree of freedom. The dimensions of the T-shaped fitting were designed to provide the desired stiffnesses between the stabilizer and the fin in the rolling and yawing degrees of freedom. The rudder was attached to the fin with two flexure hinges (fig. 3(a)) and the rotational stiffness of the rudder was controlled by a rod which extended down along the hinge line. The rod was welded at the bottom end to a fitting which was attached to the fin root.

Figure 4 is an exploded view photograph of a model of reference 1 which differed externally from the models of the present investigation principally in that the model mounting block was split into two halves. Also the attachment of the fuselage flexibility fixture to the mounting block was different. As figure 4 shows, the fin was attached to a steel tongue which in turn was attached to a steel fuselage flexibility fixture. The fuselage flexibility fixture was designed to simulate the stiffnesses of the airplane fuselage in side bending, vertical bending, and torsion. Near its upstream end the fuselage flexibility fixture was notched on all four sides to form a spring which was rectangular in cross section. The upstream end of the fuselage flexibility fixture was bolted to the model mounting block. At the downstream end a thin beam-type spring (not shown in fig. 4) connected the downstream end of the fuselage flexibility fixture to the model mounting block. The upstream spring provided the majority of the required stiffness in side bending and torsion and both upstream and downstream springs contributed to the required stiffness in vertical bending. A cylindrical lead and brass weight was suspended below the fuselage flexibility fixture. (See fig. 2.) The masses of the steel tongue, the fuselage flexibility fixture, and the lead and brass weight all contributed to the effective mass of the model fuselage.

Physical Properties

Natural vibration frequencies, stiffness properties, and mass properties of the models are presented in tables III to V, respectively; the scaled airplane properties (airplane scaled to model) are also presented for comparison. Table III contains only those measured frequencies which correspond to scaled airplane values; a complete record of the measured and required frequencies and node lines is presented in figure 5. Table IV contains all the measured and required stiffness data except the fin stiffness distributions which are presented in figure 6 in the form of fin flexibility distributions.

It was prohibitively difficult to simulate in one model configuration both the symmetric and antisymmetric frequencies and stiffnesses.

Consequently, for a given test run, the model configuration acceptably simulated either the scaled airplane symmetric or antisymmetric properties but not both. The following table shows the properties simulated during the various runs:

Airplane properties simulated	Pitch stiffness	Model	Tunnel runs
Symmetric	Normal	6	2 to 7
Antisymmetric	Normal	5	13 to 18
Symmetric	Emergency	6	8 to 11
Symmetric	Emergency	5	19 to 22

Although the model configurations tested were either symmetric or antisymmetric, both symmetric and antisymmetric properties were measured in order to define the models properly. These data are presented in tables III and IV and a code is used in tables III and IV(e) to indicate in each run the type of configuration tested.

Natural vibration frequencies.- The measured natural vibration frequencies and node lines presented in table III and figure 5 were obtained with the use of an electromagnetic shaker to excite the model. Sand crystals sprinkled on the model surface during excitation were used to define the node lines. At some natural frequencies the node lines were indistinct or could not be obtained at all. Many of the modes were highly coupled so that they involved motion in more than one degree of freedom; therefore, a description of the predominant motion is included in table III and figure 5.

One antisymmetric model configuration, model 5 with normal pitching stiffness, was investigated (tunnel runs 13 to 18). Examination of the antisymmetric frequencies and node lines for this configuration in table III and figure 5(d) shows that the antisymmetric model frequencies closely approximate the scaled airplane values, except that the model stabilizer antisymmetric torsion frequency was somewhat high. A comparison of figures 5(d) and 5(g) shows that five antisymmetric modes were obtained on the model that were not measured on the airplane. The four highest of these modes were coupled fin-rudder or coupled rudder modes which were unimportant in the flutter mode. The lowest measured model mode was the fundamental side bending of the model fuselage flexibility fixture at approximately 35 cycles per second for all models. This

[REDACTED]

vibration mode might be considered to approximate the motion of the airplane fuselage undergoing a pure side translation. The models were so designed that the second side bending frequency of the model fuselage flexibility fixture corresponds to the fundamental fuselage side bending frequency of the airplane.

The remainder of the model configurations are symmetric. As table III and figure 5 show, the model symmetric frequencies closely approximate the scaled airplane values except for the stabilizer pitch-torsion mode. On the airplane with normal pitch stiffness a single mode with a scaled frequency of 368 cycles per second was measured. No frequency was available for the airplane with emergency pitch stiffness but the value was estimated to be 305 cycles per second. (See table III.) The models had separate pitch and torsion modes which were highly coupled so that for some configurations doubt exists as to which mode was predominantly pitch and which predominantly torsion. For the models with normal pitch stiffness the frequencies of both modes were lower than the scaled airplane frequency of 368 cycles per second and for the models with emergency pitch stiffness the frequencies of the pitching mode were decreased from the values with normal pitch stiffness. For each model configuration one or two higher stabilizer symmetric modes were measured than were measured on the airplane (fig. 5).

Stiffness properties.- All measured and required stiffness data on the models except the fin stiffness distributions are given in table IV. The bending and torsion stiffnesses of the stabilizer and fins (tables IV(a) and IV(b)), the rotation and torsion stiffnesses of the rudders (table IV(c)), the side bending, vertical bending, and torsion of the fuselages (table IV(d)), and the stiffnesses of the stabilizer-fin juncture (table IV(e)) for the configurations tested were measured by standard methods. The distributions of fin flexibility in torsion and bending for the models are given in figure 6. These data were obtained by applying moments on the stabilizer (yawing moment for torsion and rolling moment for bending) and measuring the angular displacements of mirrors attached to the fin along the desired fin axes. Bending measurements were made along the reference axis (fig. 2) located along the center of airplane spar 3; torsion measurements were made along a line midway between the reference axis and the rudder hinge line. The overall fin flexibilities (values of fin flexibility at zero vertical distance from the stabilizer hinge line) are the reciprocals of the overall fin stiffnesses given in table IV(b). Differences at the top of the fin between the stabilizer rolling flexibility and the fin side bending flexibility (see fig. 6(a)) are the stabilizer-fin juncture roll-roll flexibilities. These values are the reciprocals of the roll-roll juncture stiffnesses given in table IV(e). The values of the stabilizer yaw-yaw flexibility (fig. 6(b)) are similarly related to the yaw-yaw juncture stiffnesses.

[REDACTED]

By examining tables IV(b) to IV(e) a comparison of the measured with required values of the antisymmetric stiffnesses on the one antisymmetric configuration, model 5 with normal pitch stiffness, may be made. The measured overall fin bending and torsion stiffnesses agreed well with the required values (table IV(b)). The distribution of fin flexibility is shown in figure 6 to be in good agreement with the airplane in fin bending but in somewhat less agreement in fin torsion. The rudder rotational stiffness was low and the torsion stiffness was about double the required value (table IV(c)). The fuselage side bending displacement and slope were in poor agreement with the scaled values (table IV(d)). This poor agreement was expected since on the model the second side bending frequency was used to simulate the airplane side bending mode. Also on model 5 with normal pitch stiffness, the fuselage torsion values were low (table IV(d)). The roll-roll juncture stiffness (table IV(e)) was lower than that required and the yaw-yaw value higher than that required. The roll-yaw juncture stiffness had a finite value but was acceptably large in comparison with other juncture stiffnesses.

The symmetric stiffnesses measured on the symmetric model configurations (tables IV(a), IV(d), and IV(e)) were as follows. The stabilizer bending and torsion stiffnesses, at the 71-percent-semispan position, were measured only on model 6 (table IV(a)); for this model the torsion stiffnesses were in good agreement with the airplane value whereas the bending stiffness at this station was in good agreement on the left panel, but too low on the right panel. The fuselage vertical bending stiffnesses (table IV(d)) were in fair agreement with the scaled airplane values for the symmetric configurations. The pitch-pitch juncture stiffnesses (table IV(e)) were in very good agreement with the airplane values (the value was controllable by sliding the pitch spring).

Mass properties.- Extensive mass data were obtained only on model 6 since model 5 was damaged by flutter. These data are presented in table V together with the corresponding scaled airplane data available. The mass, the static unbalance, and the desired mass moments of inertia for the stabilizer, fin, rudder, and fin with rudder are given in tables V(a) to V(d), respectively. The distributions of mass, static unbalance, and moment of inertia along the stabilizer and fin, respectively, are given in tables V(e) and V(f). These data were obtained by cutting the stabilizer and fin into streamwise strips and measuring the desired data on each strip.

The mass data on the stabilizer (table V(a)) and the mass distribution data on the stabilizer sections (table V(e)), measured on model 6, are in fair agreement with the airplane scaled values. The stabilizer mass is 9 percent too low; the static unbalance in pitch is about 3 times the airplane value; and the moments of inertia in roll, pitch, and yaw are 15 percent too high, 14 percent too low, and 7 percent too high, respectively (table V(a)). In mass distribution (table V(e)) the

stabilizer inboard sections (section 1) containing a streamline vertical fairing called the comb were too low in mass, static unbalance, and moment of inertia, the middle sections (sections 2, 3, and 4) were too high, and the outboard sections (section 5) were too low in these quantities. As previously mentioned, the lower part of the model fin leading edge was arbitrarily curved downward and terminated whereas on the airplane the fin leading edge is curved and extends forward to the canopy to form a long dorsal fin. Consequently, the mass data on the model fin (table V(b)) and the fin-section mass distribution data (table V(f)) show some discrepancies between model and scaled airplane data. The rudder alone is too high in mass and moment of inertia about the hinge line (table V(c)).

APPARATUS AND TESTS

The investigation was made in the Langley transonic blowdown tunnel which has a slotted test section that is octagonal in cross section and measures $26\frac{1}{4}$ inches between opposite sides. The tunnel Mach number is controlled by an orifice which has a variable opening and is located downstream of the tunnel test section. During operation of the tunnel the area of the orifice may be fixed at a given value. Then, as the stagnation pressure (and thus the density) is increased, the test section Mach number increases until the orifice becomes choked. Thereafter, as the stagnation pressure is increased, the Mach number remains approximately constant.

The static-density range is approximately 0.001 to 0.012 slug per cubic foot and Mach numbers from subsonic values to a maximum of about 1.4 may be obtained. It should be noted that because of the expansion of the air in the reservoir during a run, the stagnation temperature continually decreases so that the test-section velocity is not uniquely defined by the Mach number. Additional details of the tunnel are contained in reference 3. Excellent agreement between flutter data obtained in the tunnel and in free air has been observed (ref. 4).

In the present investigation the model was mounted in an inverted position on a sting fuselage that extended upstream into the subsonic flow region of the tunnel (fig. 7). This arrangement prevented the formation of shock waves off the fuselage nose which might reflect from the tunnel walls onto the model. The sting consisted of two 3-inch-diameter tubes fitted one above the other as indicated in figure 7. The lower tube accommodated the fuselage block (fig. 1), and the upper tube shielded the weight which was attached to the fuselage flexibility fixture (fig. 4). The sting and model weighed approximately 310 pounds, and the system had a fundamental bending frequency of about 15 cycles per second.

Wire strain gages were mounted on the main spar of the fin near the root (fig. 3(a)) and on one side of the stabilizer near the stabilizer-fin juncture (fig. 3(b)). Each set of these gages was oriented to indicate deflections about two different axes. A strain gage to indicate rudder rotation was mounted on a thin metal strip which was bent in a shallow arc, placed so as to span the rudder hinge line, and glued at one end to the rudder and the other end to the fin (fig. 3(a)).

The strain-gage signals, the tunnel stagnation and the static pressures, and the stagnation temperature were recorded on a recording oscillograph. The strain-gage signals were used to indicate the start of flutter and the flutter frequency. High-speed motion pictures were made during the runs and used to detect the type of flutter mode.

An optical system displayed an image of the model on a ground-glass screen during the runs. The image was watched carefully in an attempt to observe flutter and to stop the air flow before the model became damaged. For the same purpose, the strain-gage outputs were viewed on the recording oscillograph.

Since the models had somewhat less than scaled strength, it was necessary to orient them with the tunnel airstream in order to avoid excessive static loadings that might destroy the models. The model was considered to be trimmed in angle of attack when zero symmetric deflection of the stabilizer tips was observed and to be trimmed in angle of yaw when zero antisymmetric deflection of the stabilizer tips was observed. A trim run on each model (runs 1 and 12) was necessary to determine the proper orientation of the model in the tunnel airstream.

RESULTS AND DISCUSSION

Interpretation of Data

As stated in the section entitled "Scaling," a stiffness reduction factor of 76 percent was applied in scaling the airplane stiffness. The simulated altitudes indicated in figure 8 are thus to be interpreted as altitudes which, if cleared by the model, could be reached with a 32 per-

cent $\left(\frac{1}{0.76} = 1.32\right)$ margin of safety in stiffness by the airplane. This statement assumes, of course, that the model in all other respects exactly simulates the airplane. An alternate interpretation of the results is that a flutter point obtained with the model indicates that the airplane will flutter at the same Mach number at a simulated altitude corresponding to a dynamic pressure 32 percent greater than the dynamic pressure at model flutter.

Presentation of Data

A compilation of the wind-tunnel results is presented in table VI and the data points given in this table are plotted in figure 8 in the form of dynamic pressure as a function of Mach number. Three types of data points are presented in table VI and figure 8. If flutter or a phenomenon called low damping occurred during a run, the data point corresponding to the start of flutter or start of low damping is presented. If no flutter occurred, the point of maximum dynamic pressure obtained during the run is given.

During some of the runs intermittent bursts of nearly sinusoidal oscillations were obtained. It is believed that for this condition the damping was low but not zero. Selection of the start of a low damping region was somewhat arbitrary because the start of low damping was indefinite. The relationship of the low damped oscillations of the model in the wind tunnel to the behavior of the airplane in free air is not known.

Discussion of Results

Antisymmetric flutter.- The only model configuration applicable to antisymmetric flutter was model 5 as investigated in runs 13 to 18. As shown in figure 8(a) the model did not flutter although the maximum dynamic pressure exceeded that of the scaled airplane flight boundary by 35 percent at a Mach number of 0.80, 29 percent at a Mach number of 0.93, and, by interpolation, 10 percent at a Mach number of 1.05. Thus, if differences between the measured model and scaled airplane properties are disregarded, the airplane is indicated to have an adequate margin of safety from antisymmetric flutter at transonic Mach numbers.

The fin torsional frequency of the model investigated was too high by 6 percent (table III(a)). Often for T-tails, the dynamic pressure for antisymmetric flutter varies approximately as the fin torsional stiffness (ref. 5) or as the square of the fin torsional frequency. If it is assumed that such a variation is applicable to the present case, the dynamic pressures indicated in figure 8(a) would be reduced by about 11 percent. Application of this correction would still leave three of the data points in figure 8(a) at dynamic pressures higher than those for the scaled airplane flight boundary and spaced so as to cover the Mach number range of the tests.

Other possibly important model deficiencies include (table IV(e)) a yaw-yaw juncture stiffness which was too high by 23 percent and a roll-roll juncture stiffness which was too low by 34 percent. The effects of these deficiencies in juncture stiffnesses on the flutter characteristics are not known.

Symmetric flutter, normal pitching stiffness.- The only model configuration with a normal value of stabilizer pitching stiffness which was applicable to symmetric flutter was model 6 as investigated in runs 2 to 7. As shown in figure 8(b) the model did not flutter although the maximum dynamic pressures exceeded those of the scaled flight boundary by a slight amount throughout the Mach number range investigated. Thus, if differences between the measured model and scaled airplane properties are disregarded, the airplane with the normal pitching stiffness is indicated to have an adequate safety margin from symmetric flutter at transonic Mach numbers.

It should be noted (table IV(e)) that the model stabilizer pitching stiffness was very close to the scaled airplane value. However, the model stabilizer moment of inertia about the pitch axis (table V(a)) was too low by 14 percent and the model stabilizer pitching frequency was too low by 8 percent (table III(b)). (Note in table III(b) that whereas the models had distinct stabilizer torsion and pitching natural vibration modes, the airplane had a coupled stabilizer torsion-pitch mode.) If it is assumed that the dynamic pressure for flutter is proportional to the product of the stabilizer pitching inertia and the square of the stabilizer fundamental pitching frequency, the dynamic pressure of the data points in figure 8(b) would be corrected to values 36 percent higher than shown. The assumption is based on the fact that the flutter mode for the case of emergency pitching stiffness (to be discussed subsequently) involved predominantly stabilizer pitching motion. The assumption is also based on the approximate flutter formula given in reference 6 with the stabilizer pitching frequency substituted for the torsion frequency.

Another difference between measured model and scaled airplane properties, as may be determined from table V(a), is that the model center of gravity was too far rearward by 4 percent of the stabilizer center-line chord. The approximate flutter formula of reference 6 indicates that a correction for this difference would raise the dynamic pressures for the data points in figure 8(b) to even higher values.

Symmetric flutter, emergency pitching stiffness.- The two model configurations with emergency values of stabilizer pitching stiffness which were applicable to symmetric flutter were model 6 as investigated in runs 8 to 11 and model 5 as investigated in runs 19 to 22. As shown in figure 8(c), symmetric flutter was obtained on both models. The flutter obtained with model 6 occurred at lower dynamic pressures than it did for model 5; this resulted in scatter in the flutter points. However, the flutter obtained with model 5 was preceded by relatively long periods of low damping. The flutter points obtained at the lower values of dynamic pressure occurred within the flight boundary at 785 feet altitude at a Mach number of 0.89 and at 5,690 feet altitude at a Mach number of 1.01. Thus, if differences between the measured model and scaled airplane properties are disregarded, the airplane with the emergency stabilizer

[REDACTED]

pitching stiffness is indicated not to have the required stiffness margin of safety at Mach numbers above about 0.85 at low altitudes.

Examination of the high-speed motion pictures and oscillograph records obtained during the testing disclosed that the flutter mode for both models involved predominantly stabilizer pitching motion coupled with some stabilizer fundamental bending. The frequency of flutter (table VI) was 186 and 197 cycles per second for model 6, and 214 cycles per second for model 5. These flutter frequencies fall above the fundamental bending frequency and below the measured pitch and torsion frequencies of the models. On model 6 the rudder strain-gage installation was faulty and no information on the rudder motion was obtained; however, the motion-picture data on both models and the strain-gage data from model 5 indicated that rudder motion did not play a significant part in the flutter mode. No antisymmetric fin bending or torsion motion, or fuselage side bending or rotational motion, were excited during the flutter. Furthermore, no fuselage vertical bending motion could be detected from the motion pictures until after the flutter was well established and the dynamic pressure increased beyond the start-of-flutter value.

As indicated in table IV(e), the model stabilizer pitching stiffnesses were very close to the scaled airplane value. However, the model stabilizer pitching frequency (table III(b)) varied from 6 percent lower than the scaled airplane value to 2 percent higher than the scaled airplane value, and the moment of inertia about the pitch axis (table V(a)) was 14 percent lower than the scaled airplane value. Correction of the data for the differences between the actual and the scaled airplane values of stabilizer pitching frequency and stabilizer moment of inertia, as discussed for the case of symmetric flutter with normal pitching stiffness, raises the dynamic pressures for the flutter points shown in figure 8(c) by from 12 to 31 percent; based on this correction, the airplane should have an adequate margin of safety from flutter within the airplane flight boundary.

Limitations of results.- It should be noted that the lower part of the model fin leading edge (figs. 1 and 2) extended forward some distance ahead of the stabilizer. Therefore, the possibility exists that shock waves from the fin could reflect from the walls back to the model at Mach numbers above 1.00. Thus, data obtained above a Mach number of 1.00 may be open to some question.

The corrections to the symmetric-flutter results, as discussed previously, are based on the approximate flutter formula of reference 6 and may not be applicable in the present cases. It is recognized that a better method for correcting the experimental data would be based on the results of more refined flutter calculations. In such a method the experimental dynamic pressures would be multiplied by the ratio of flutter dynamic pressures calculated using required model properties to flutter

[REDACTED]

dynamic pressures calculated using the actual model properties. No such refined flutter calculations have been made for the present report.

CONCLUSIONS

A transonic flutter investigation of models of the T-tail of the Blackburn NA-39 airplane has resulted in the following conclusions:

1. If differences between the measured model properties and the scaled airplane properties are disregarded, the airplane with the normal value of stabilizer pitching stiffness should have a stiffness margin of safety from both symmetric and antisymmetric flutter of at least 32 percent at all Mach numbers and altitudes within the flight boundary. However, the airplane with the emergency value of stabilizer pitching stiffness would not have the required margin of safety from symmetrical flutter at Mach numbers greater than about 0.85 at low altitudes.

2. First-order corrections for some differences between the measured model properties and the scaled airplane properties indicated that the airplane with the normal value of stabilizer pitching stiffness would still have an adequate margin of safety from flutter and that the flutter safety margin for the airplane with the emergency value of stabilizer pitching stiffness would be changed from inadequate to adequate. However, the validity of the corrections is questionable.

Langley Research Center,
National Aeronautics and Space Administration,
Langley Field, Va., November 17, 1959.

REFERENCES

1. Jones, George W., Jr., and Boswinkle, Robert W., Jr.: Preliminary Transonic Flutter Investigation of Models of T-tail of Blackburn NA-39 Airplane. NACA RM SL58D10, Office Naval Res., 1958.
2. Anon.: Standard Atmosphere - Tables and Data for Altitudes to 65,800 Feet. NACA Rep. 1235, 1955. (Supersedes NACA TN 3182.)
3. Unangst, John R., and Jones, George W., Jr.: Some Effects of Sweep and Aspect Ratio on the Transonic Flutter Characteristics of a Series of Thin Cantilever Wings Having a Taper Ratio of 0.6. NACA RM L55I13a, 1956.
4. Bursnall, William J.: Initial Flutter Tests in the Langley Transonic Blowdown Tunnel and Comparison With Free-Flight Flutter Results. NACA RM L52K14, 1953.
5. Land, Norman S., and Fox, Annie G.: An Experimental Investigation of the Effects of Mach Number, Stabilizer Dihedral, and Fin Torsional Stiffness on the Transonic Flutter Characteristics of a Tee-Tail. NACA RM L57A24, 1957.
6. Theodorsen, Theodore, and Garrick, I. E.: Mechanism of Flutter - A Theoretical and Experimental Investigation of the Flutter Problem. NACA Rep. 685, 1940.

TABLE I.- GEOMETRIC CHARACTERISTICS OF MODELS

Stabilizer:

Aspect ratio	2.64
Sweepback of leading edge, deg	29
Sweepback of trailing edge, deg	9
Taper ratio	0.582
Maximum thickness at center line, percent center-line chord	5
Maximum thickness at tip, percent streamwise tip chord	5
Center-line chord, ft	0.559
Span, ft	1.170
Area, sq ft	0.518
Pitch axis, percent center-line chord	52

Fin-rudder:

Sweepback of trailing edge, deg	22
Maximum root thickness, percent streamwise root chord	11
Maximum thickness at minimum streamwise chord, percent minimum streamwise chord	8
Streamwise root chord, ft	1.08
Minimum streamwise chord, ft	0.56
Area, (not including lateral area of stabilizer), sq ft	0.45
Height of stabilizer above fin-rudder root chord, ft	0.57
Sweepback of leading edge of main spar, deg	27

Rudder:

Sweepback of hinge line, deg	22
Streamwise chord, ft	0.17
Rudder span (perpendicular to fuselage center line), ft	0.45
Area, sq ft	0.076

Fuselage:

Diameter, ft	0.25
------------------------	------

TABLE II.- DESIGN SCALE FACTORS OF PERTINENT
MODEL AND FLOW QUANTITIES

$$\left[\frac{\rho_M}{\rho_A} = 1.97; \frac{T_M}{T_A} = 0.786; \lambda = 0.76 \right]$$

Quantity	Design scale factor	
	Symbolical	Numerical
Fundamental quantities:		
Length	l	$\frac{1}{12}$
Mass	$m = \frac{\rho_M}{\rho_A} l^3$	1.14×10^{-3}
Time	$t = \left(\frac{T_M}{T_A} \right)^{-0.5} l$	0.940×10^{-1}
Derived quantities:		
Stream velocity	lt^{-1}	0.887
Stream dynamic pressure	$ml^{-1}t^{-2}$	1.55
Moment of inertia	ml^2	0.792×10^{-5}
Natural vibration frequencies	$\lambda^{0.5}t^{-1}$	9.27
Angular deflections divided by applied moment	$\lambda^{-1}l^{-2}m^{-1}t^2$	1,470
Applied force divided by displacement	λmt^{-2}	0.981×10^{-1}
Applied moment divided by angular deflection	$\lambda mt^{-2}l^2$	0.681×10^{-3}
Applied force divided by slope	$\lambda mt^{-2}l$	0.817×10^{-2}
Mass unbalance	ml	0.950×10^{-4}

TABLE III.- MODEL NATURAL VIBRATION FREQUENCIES

(a) Antisymmetric modes

Configuration (a)	Model	Runs	Frequency, cps					
			Fin bending, stabilizer in phase	Fin torsion, stabilizer in phase	Fin bending, stabilizer out of phase	Fuselage side bending	Rudder rotation	Stabilizer torsion
SN	6	2 to 7	56	70	94	117	169	370
SE	6	8 to 10	57	73	99	123	171	371
SE	6	11	58	72	99	124	170	369
AN	5	13 to 18	58	73	102	127	175	395
SE	5	19 to 21	55	71	98	118	167	395
SE	5	22	55	71	98	116	167	395
Scaled airplane properties			57	69	99	125	164	345

(b) Symmetric modes

Configuration (a)	Model	Runs	Frequency, cps			
			Fuselage vertical bending	Stabilizer fundamental bending	Stabilizer torsion	Stabilizer pitching
SN	6	2 to 7	106	170	275	339
SE	6	8 to 10	110	170	260	301
SE	6	11	111	166	260	287
AN	5	13 to 18	143	193	268	328
SE	5	19 to 21	108	171	290	310
SE	5	22	105	179	299	308
Scaled airplane properties			108	171	^b 368 (normal) ^c 305 (emergency)	

^aCode: S, symmetric model; A, antisymmetric model; N, normal pitching stiffness; E, emergency pitching stiffness.

^bStabilizer torsion-pitching frequency.

^cStabilizer emergency pitching frequency obtained by multiplying normal frequency by the square root of the ratio of required emergency pitch stiffness to normal pitch stiffness.

TABLE IV.- MODEL STIFFNESSES

(a) Stabilizers

Model	Panel	Runs	Bending (vertical force at 35 percent chord at station 60 (71 percent semispan) with center-line chord restrained divided by vertical displacement at same point), lb/ft	Torsion (twisting moment applied about lateral line at station 60 (71 percent semispan) with center-line chord restrained divided by streamwise angular deflection at station 60), ft-lb/radian
6	Left Right	2 to 11	5.03×10^3 3.14	0.293×10^3 .260
Scaled airplane properties			5.77×10^3	0.292×10^3 (symmetric) .281 (antisymmetric)

(b) Fins

Model	Runs	Bending (twisting moment applied through stabilizer to spar 3 with fin root restrained divided by slope at top of spar 3), ft-lb/radian	Torsion (twisting moment applied through stabilizer about line halfway between spar 3 and rear spar with fin root restrained divided by angular deflection at top of line), ft-lb/radian
6 5	2 to 11 13 to 22	0.532×10^3 .568	0.581×10^3 .675
Scaled airplane properties		0.562×10^3	0.630×10^3

TABLE IV.- MODEL STIFFNESSES - Continued

(c) Rudders

Model	Runs	Rotation (moment applied about hinge line divided by angular deflection of rudder root chord in direction normal to hinge line), ft-lb/radian	Torsion (moment applied at tip about hinge line with root restrained divided by rotation of tip in direction normal to hinge line), ft-lb/radian
6 5	2 to 11 13 to 22	6.18 5.33	25.02 25.22
Scaled airplane properties		6.81	12.12

(d) Fuselage (all loads and deflections were applied and measured at station 562.5)

Model	Runs	Side bending (a)		Vertical bending		Torsion
		Side force divided by side displace- ment, lb/ft.	Side force divided by slope in yaw direction, lb/radian	Vertical force divided by vertical displacement, lb/ft	Vertical force divided by slope in pitch direction, lb/radian	Rolling moment divided by rolling deflection, ft-lb/radian
6 5 5	2 to 11 13 to 18 19 to 22	1.71×10^4 2.52 1.33	1.01×10^4 1.34 .899	12.82×10^4 22.21 9.60	6.10×10^4 23.04 15.9	0.85×10^4 .53 .63
Scaled airplane properties		7.31×10^4	7.17×10^4	9.41×10^4	7.78×10^4	1.09×10^4

^aAlthough the model side bending stiffnesses are lower than required, the second fuselage side bending frequency of the model simulates the scaled airplane first side bending frequency.

TABLE IV.- MODEL STIFFNESSES - Concluded

(e) Stabilizer-fin juncture

Model	Configuration	Runs	Roll-roll (rolling moment applied to stabilizer divided by dif- ference in rolling deflec- tion between stabilizer center line and top of fin), ft-lb/radian	Pitch-pitch (pitching moment applied to stabilizer divided by dif- ference in pitching deflec- tion between stabilizer center line and top of fin), ft-lb/radian	Yaw-yaw (yawing moment applied to stabilizer divided by dif- ference in yawing deflec- tion between stabilizer center line and top of fin), ft-lb/radian	Roll-yaw (rolling moment applied to stabilizer divided by dif- ference in yawing deflec- tion between stabilizer center line and top of fin), ft-lb/radian
6	SN	2 to 7	1.00×10^3	1.78×10^3	1.67×10^3	121.5×10^3
6	SE	8 to 10	1.73	1.24	2.00	194.0
6	SE	11	1.33	1.26	1.92	-----
5	AN	13 to 18	1.56	1.83	1.33	195.0
5	SE	19 to 21	1.15	1.26	1.25	324.0
5	SE	22	1.15	1.29	1.25	324.0
Scaled airplane properties			2.36×10^3	1.82×10^3 (Normal) 1.25 (Emergency)	1.08×10^3	Infinite

^aCode: S, symmetric model; A, antisymmetric model; N, normal pitching stiffness; E, emergency pitching stiffness.

TABLE V.- MODEL MASS DATA

(a) Stabilizers

Model	Mass, slugs	Unbalance about indicated stabilizer axes, slug-ft		Moment of inertia about axis through stabilizer center of gravity and parallel to indicated stabilizer axes, slug-ft ²		
		Roll (positive for center of gravity on right stabilizer)	Pitch (positive for center of gravity rearward)	Roll	Pitch	Yaw
6	2.15×10^{-2}	0.054×10^{-3}	0.663×10^{-3}	17.30×10^{-4}	4.39×10^{-4}	20.30×10^{-4}
Scaled airplane properties	2.37×10^{-2}	0	0.196×10^{-3}	15.00×10^{-4}	5.13×10^{-4}	18.97×10^{-4}

(b) Fins

Model	Mass, slugs	Unbalance about indicated stabilizer axes, slug-ft		Moment of inertia about axis through fin center of gravity and parallel to indicated stabilizer axes, slug-ft ²		
		Roll	Yaw (positive for center of gravity rearward)	Roll	Pitch	Yaw
6	1.84×10^{-2}	5.75×10^{-3}	-4.63×10^{-3}	8.5×10^{-4}	21.89×10^{-4}	14.80×10^{-4}
Scaled airplane properties.	1.91×10^{-2}	5.40×10^{-3}	-3.23×10^{-3}	-----	-----	7.45×10^{-4}

TABLE V.- MODEL MASS DATA - Continued

(c) Rudders

Model	Mass, slugs	Unbalance about hinge line (positive for center of gravity rearward), slug-ft	Moment of inertia about hinge line, slug-ft ²
6	12.68×10^{-4}	5.49×10^{-5}	10.40×10^{-6}
Scaled airplane properties	8.50×10^{-4}	5.32×10^{-5}	6.27×10^{-6}

(d) Fins with rudders

Model	Mass, slugs	Unbalance about indicated stabilizer axes, slug-ft		Moment of inertia about axis through fin-rudder center of gravity and parallel to indicated stabilizer axes, slug-ft ²		
		Roll	Yaw (positive for center of gravity rearward)	Roll	Pitch	Yaw
6	1.97×10^{-2}	6.20×10^{-3}	-4.59×10^{-3}	8.77×10^{-4}	23.50×10^{-4}	17.2×10^{-4}
Scaled airplane properties	2.00×10^{-2}	-----	-----	-----	-----	-----

TABLE V.- MODEL MASS DATA - Continued

(e) Model 6, stabilizer sections

Section	Airplane station, in. outboard from stabilizer center line	Panel	Mass, slugs	Unbalance about indicated stabilizer axes, slug-ft		Moment of inertia about axis through section center of gravity and parallel to stabilizer pitch axis, slug-ft ²
				Roll	Pitch (positive for center of gravity rearward)	
1	0 to 16.8	Left	4.00×10^{-3}	1.59×10^{-4}	-1.13×10^{-4}	8.74×10^{-5}
		Right	4.26	1.77	-1.49	9.44
		Scaled airplane properties	5.74	1.53	-3.22	12.01
2	16.8 to 33.6	Left	2.23×10^{-3}	3.85×10^{-4}	0.17×10^{-4}	3.50×10^{-5}
		Right	2.19	3.87	.13	3.26
		Scaled airplane properties	1.82	3.16	.03	2.59
3	33.6 to 50.4	Left	1.82×10^{-3}	5.30×10^{-4}	0.96×10^{-4}	2.55×10^{-5}
		Right	1.81	5.38	.90	2.19
		Scaled airplane properties	1.64	4.79	.62	1.84
4	50.4 to 67.2	Left	1.54×10^{-3}	6.23×10^{-4}	1.55×10^{-4}	1.83×10^{-5}
		Right	1.55	6.40	1.56	1.81
		Scaled airplane properties	1.44	5.89	1.43	1.45
5	67.2 to 84.4	Left	1.07×10^{-3}	5.60×10^{-4}	1.62×10^{-4}	1.04×10^{-5}
		Right	1.11	5.90	1.65	1.03
		Scaled airplane properties	1.22	6.47	1.92	1.19
1 to 5	0 to 84.4	Left	10.66×10^{-3}	22.57×10^{-4}	-----	-----
		Right	10.92	23.32	-----	-----
		Scaled airplane properties	11.86	21.84	0.98×10^{-4}	25.63×10^{-5}

TABLE V.- MODEL MASS DATA - Concluded

(f) Model fin sections

Section	Model	Airplane station, in. above airplane center line	Mass, slugs	Unbalance about indicated stabilizer axes, slug-ft		Moment of inertia about axis through section center of gravity and parallel to stabilizer yaw axis, slug-ft ²
				Roll	Yaw (positive for center of gravity rearward)	
1	6 Scaled airplane properties	22.4 to 40	5.90×10^{-3}	32.5×10^{-4}	-26.1×10^{-4}	36.32×10^{-5}
		20 to 40	4.01	21.6	-12.9	12.52
2	6 Scaled airplane properties	40 to 60	3.23×10^{-3}	13.0×10^{-4}	-12.3×10^{-4}	18.83×10^{-5}
		40 to 60	4.01	15.9	-11.2	14.08
3	6 Scaled airplane properties	60 to 80	3.56×10^{-3}	1.1×10^{-4}	-9.0×10^{-4}	11.57×10^{-5}
		60 to 80	4.67	12.1	-7.3	11.63
4	6 Scaled airplane properties	80 to 110.7	6.33×10^{-3}	4.9×10^{-4}	-1.64×10^{-4}	5.31×10^{-5}
		80 to 110	6.45	4.4	-9	6.41

TABLE VI.- COMPILATION OF FLUTTER DATA

Model	Configuration (a)	Run	Point	Model behavior (b)	Frequency, cps	Mach number	Dynamic pressure, $\frac{\text{lb}}{\text{sq ft}}$	Velocity, $\frac{\text{ft}}{\text{sec}}$	Density, $\frac{\text{slugs}}{\text{cu ft}}$	Static temperature, $^{\circ}\text{R}$
6	SN	2	1	Q	---	0.741	1,323	745	0.0048	421
		3	1	Q	---	.833	1,718	832	.0050	415
		4	1	Q	---	.884	1,957	882	.0050	415
		5	1	Q	---	.995	2,241	979	.0047	403
		6	1	Q	---	.961	2,192	951	.0048	407
		7	1	Q	---	1.072	2,520	1,036	.0043	389
5	SE	8	1	Q	---	0.729	1,329	756	0.0046	447
		9	1	Q	---	.814	1,663	835	.0048	438
		10	1	D	---	.891	1,688	912	.0041	436
		11	2	F	186	.899	1,803	917	.0043	433
			1	F	197	1.008	1,904	1,031	.0036	436
	AN	13	1	Q	---	0.848	1,797	850	0.0050	418
		14	1	Q	---	.910	2,045	899	.0051	406
		15	1	Q	---	1.020	2,327	993	.0047	395
		16	1	Q	---	.803	2,002	806	.0061	420
		17	1	Q	---	1.086	2,532	1,044	.0046	385
		18	1	Q	---	.927	2,569	913	.0061	404
		19	1	D	---	0.943	2,080	935	0.0048	409
	SE	20	2	F	214	.961	2,419	938	.0055	396
		21	1	Q	---	.844	1,800	868	.0048	440
		22	1	D	---	.833	2,225	859	.0060	442
			2	F	214	.827	2,635	838	.0075	428
			1	D	---	.897	2,376	906	.0058	424
			2	Q	---	.900	2,482	904	.0061	420

^aModel code: S, symmetric model; A, antisymmetric model; N, normal pitching stiffness; E, emergency pitching stiffness.

^bModel behavior code: Q, maximum dynamic pressure during tunnel run, no flutter; D, start of low damping in symmetric mode; F, start of flutter in symmetric mode.

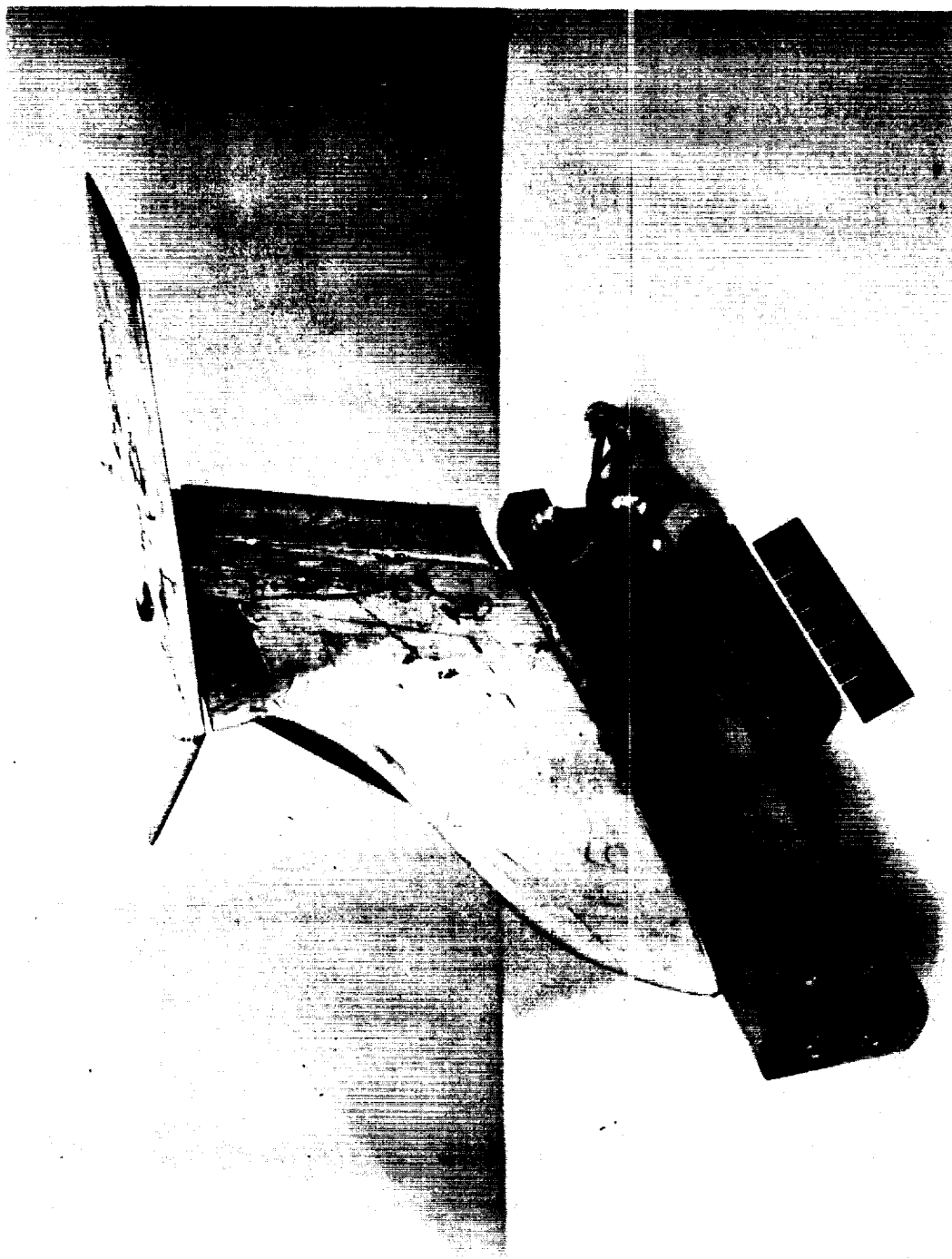


Figure 1.- Photograph of model.

L-59-2405

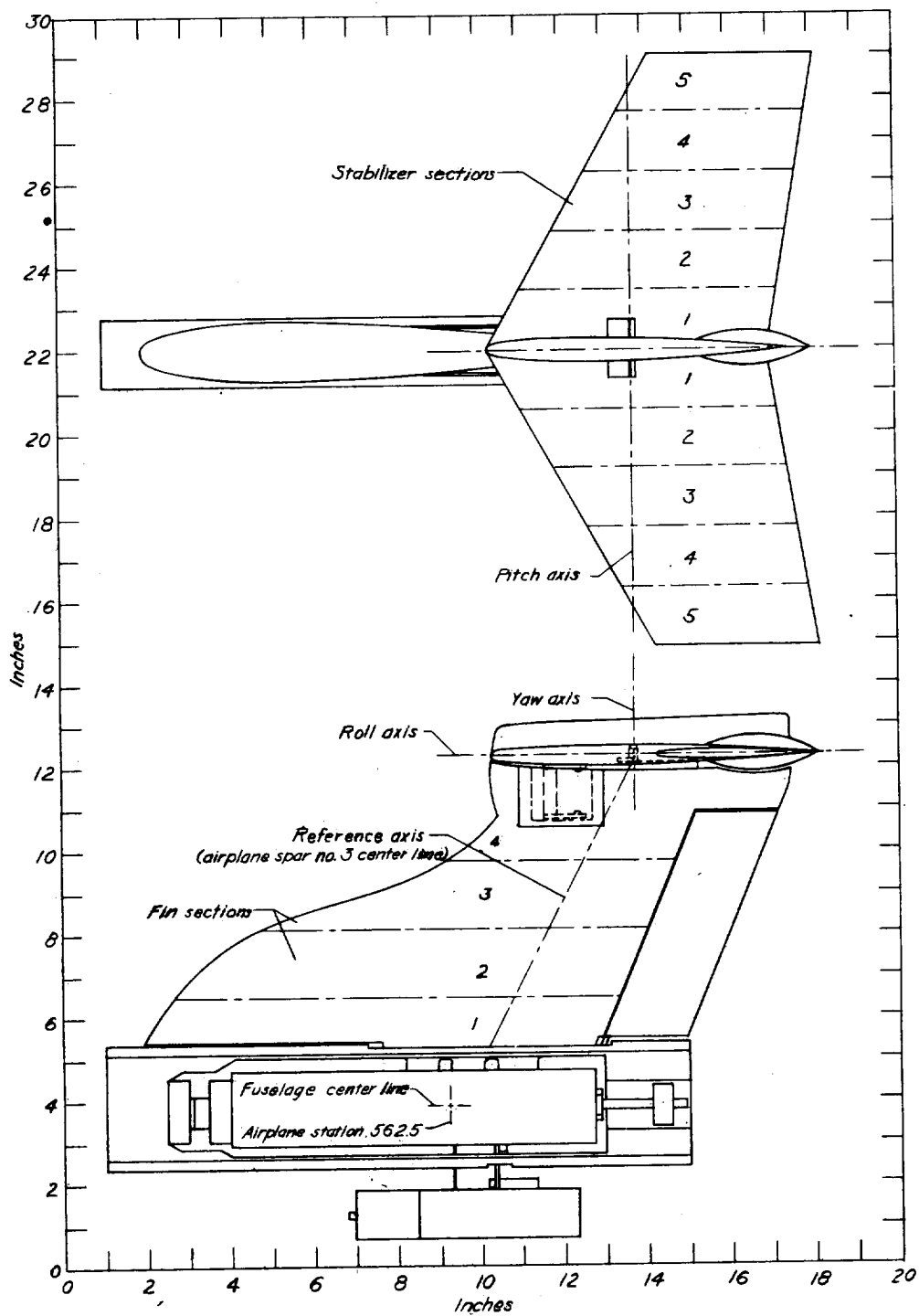
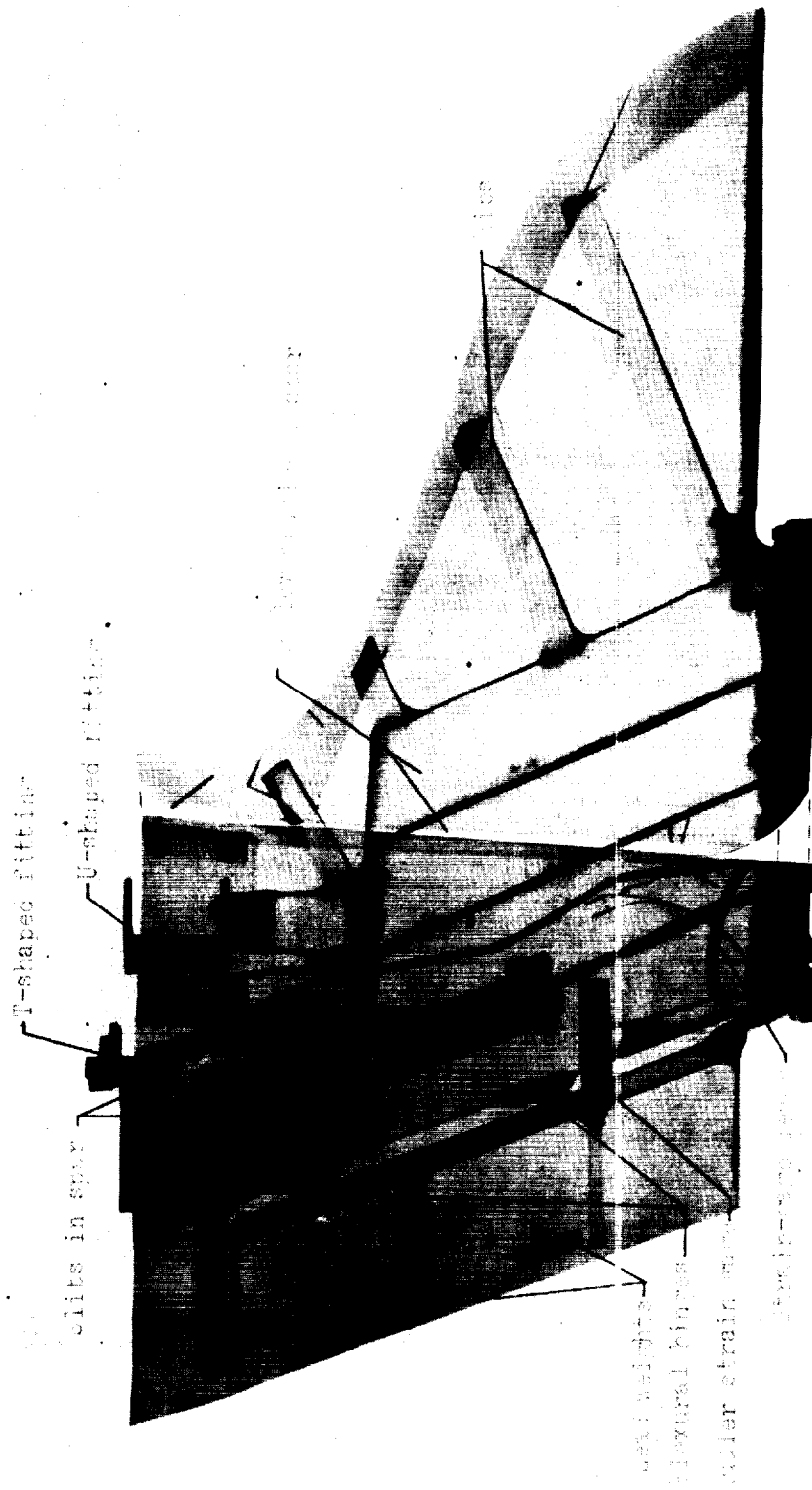


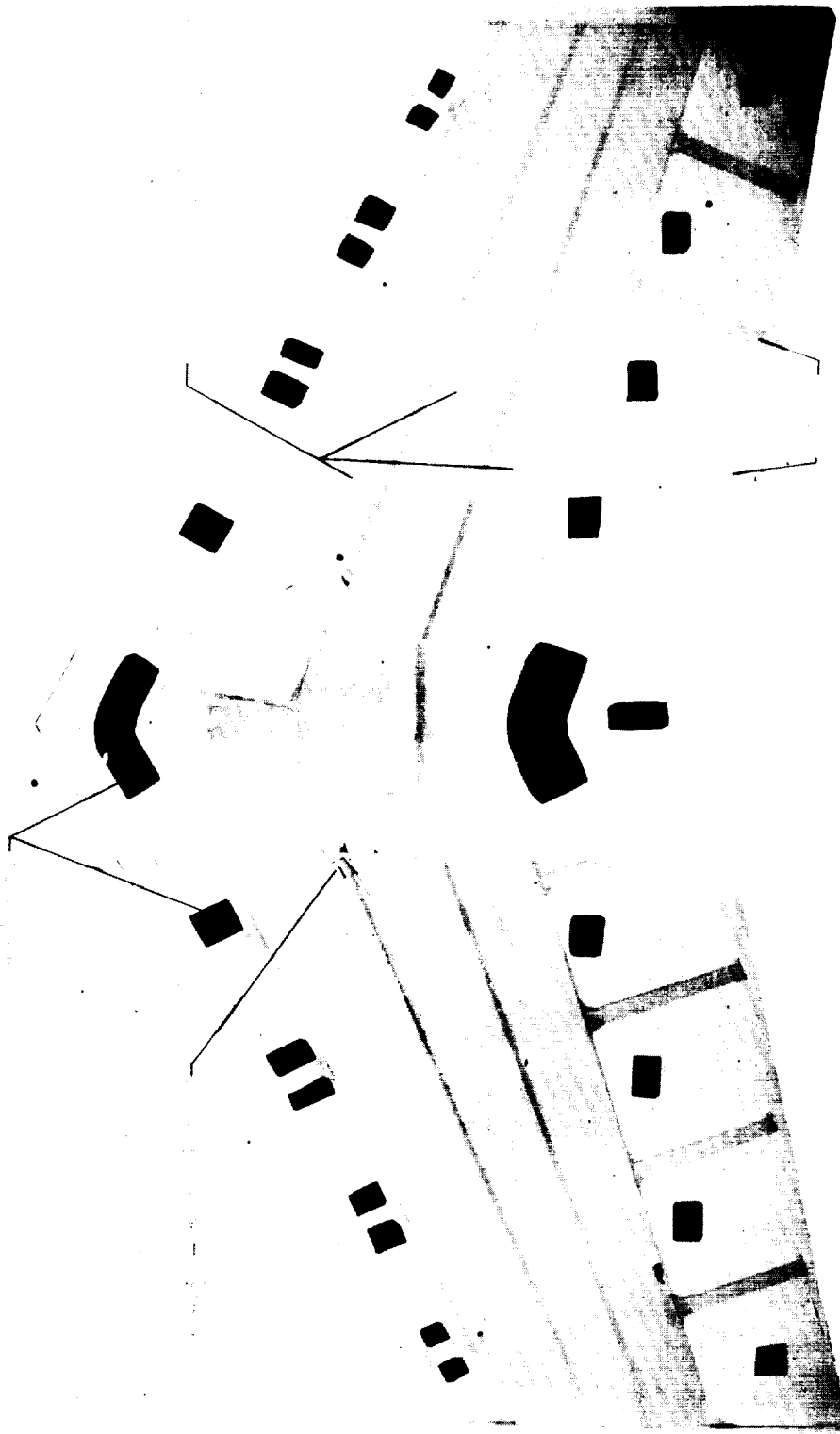
Figure 2.- Sketch of model.



(a) Model 6, fin and rudder.

L-59-6486

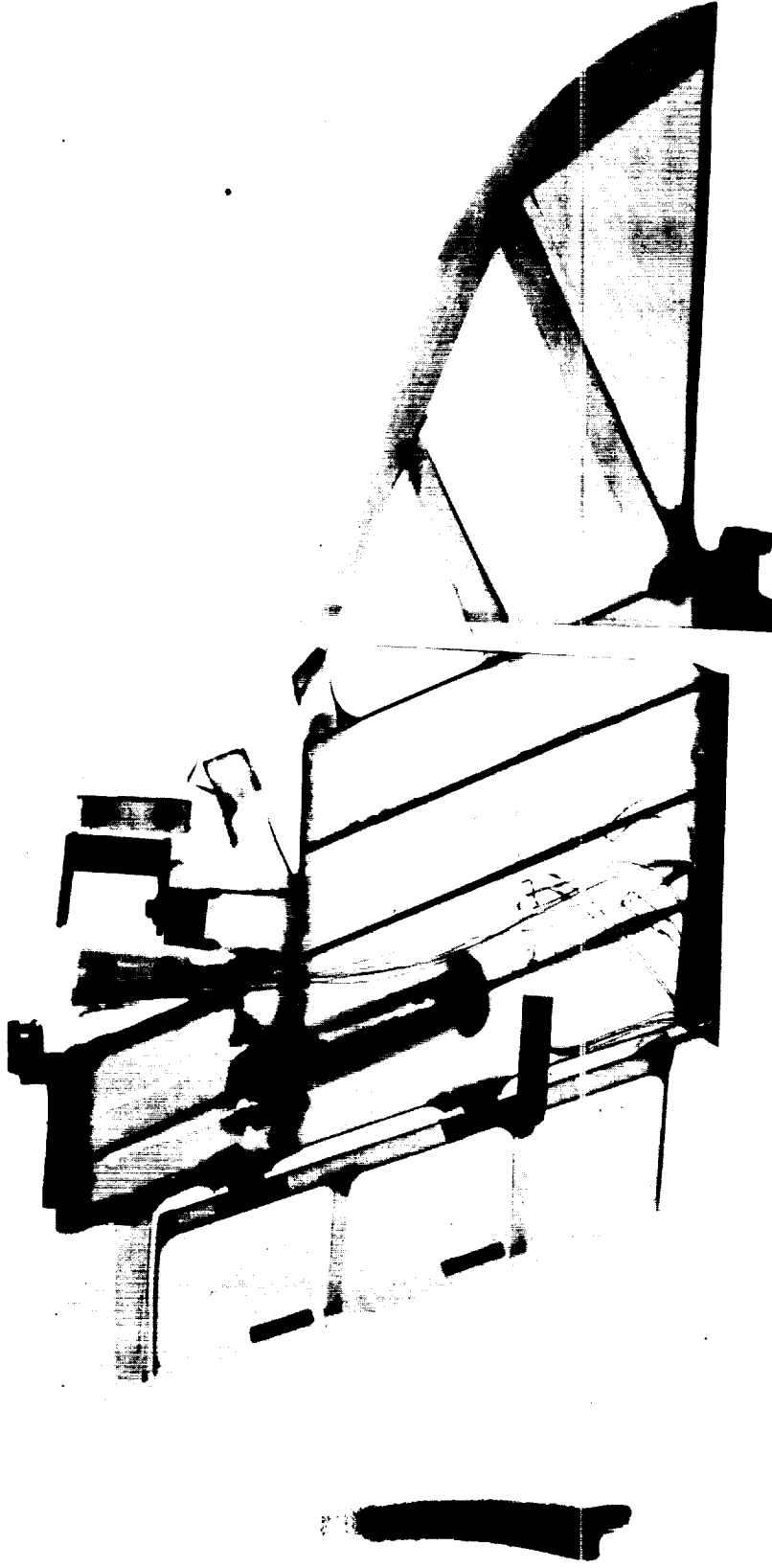
Figure 3.- Composite X-ray photographs of model.



(b) Model 6, stabilizer.

L-59-6487

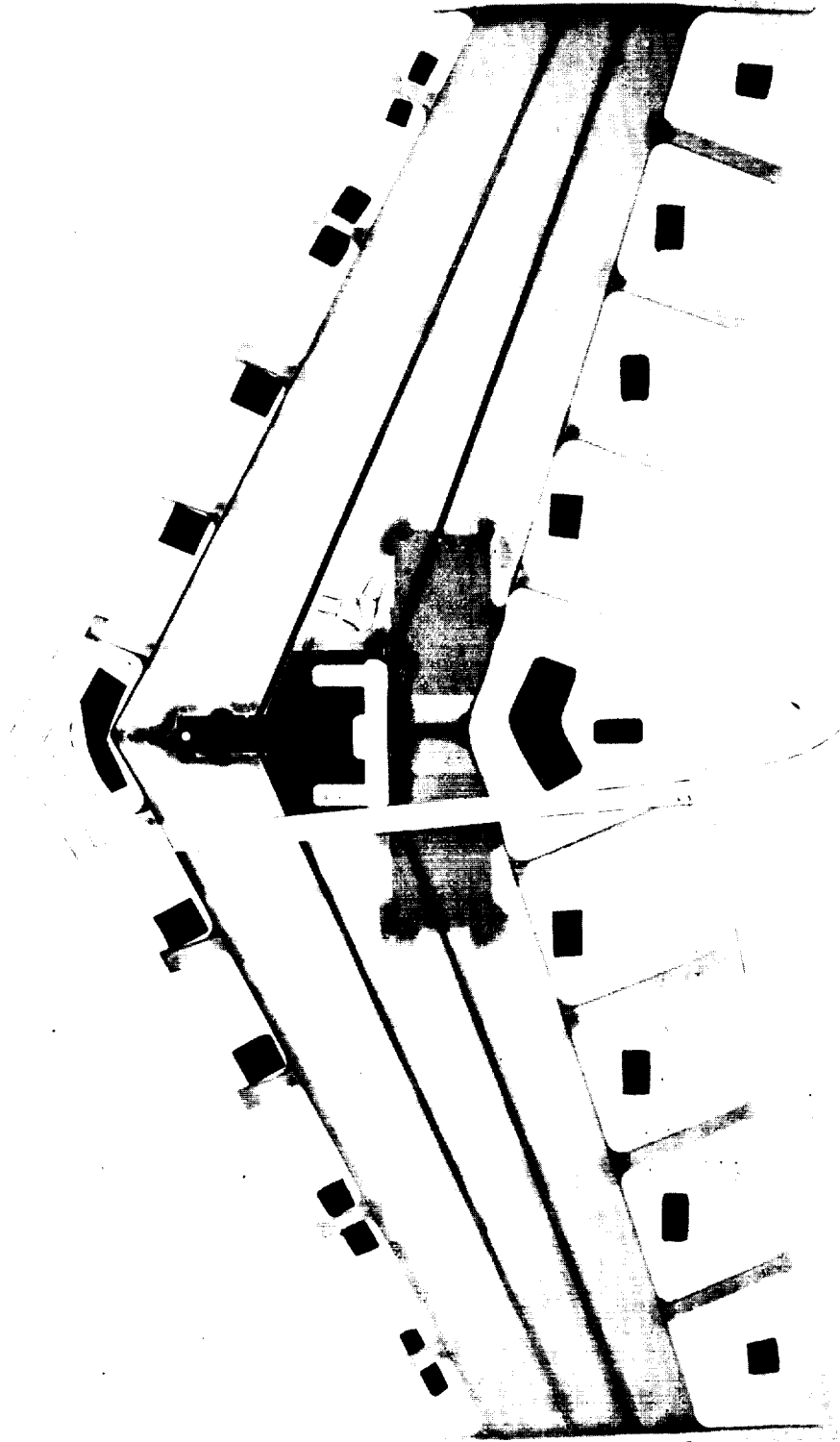
Figure 3.- Continued.



(c) Model 5, fin and rudder.

L-59-6488

Figure 3.- Continued.



(d) Model 5, stabilizer.

L-59-6489

Figure 3.- Concluded.

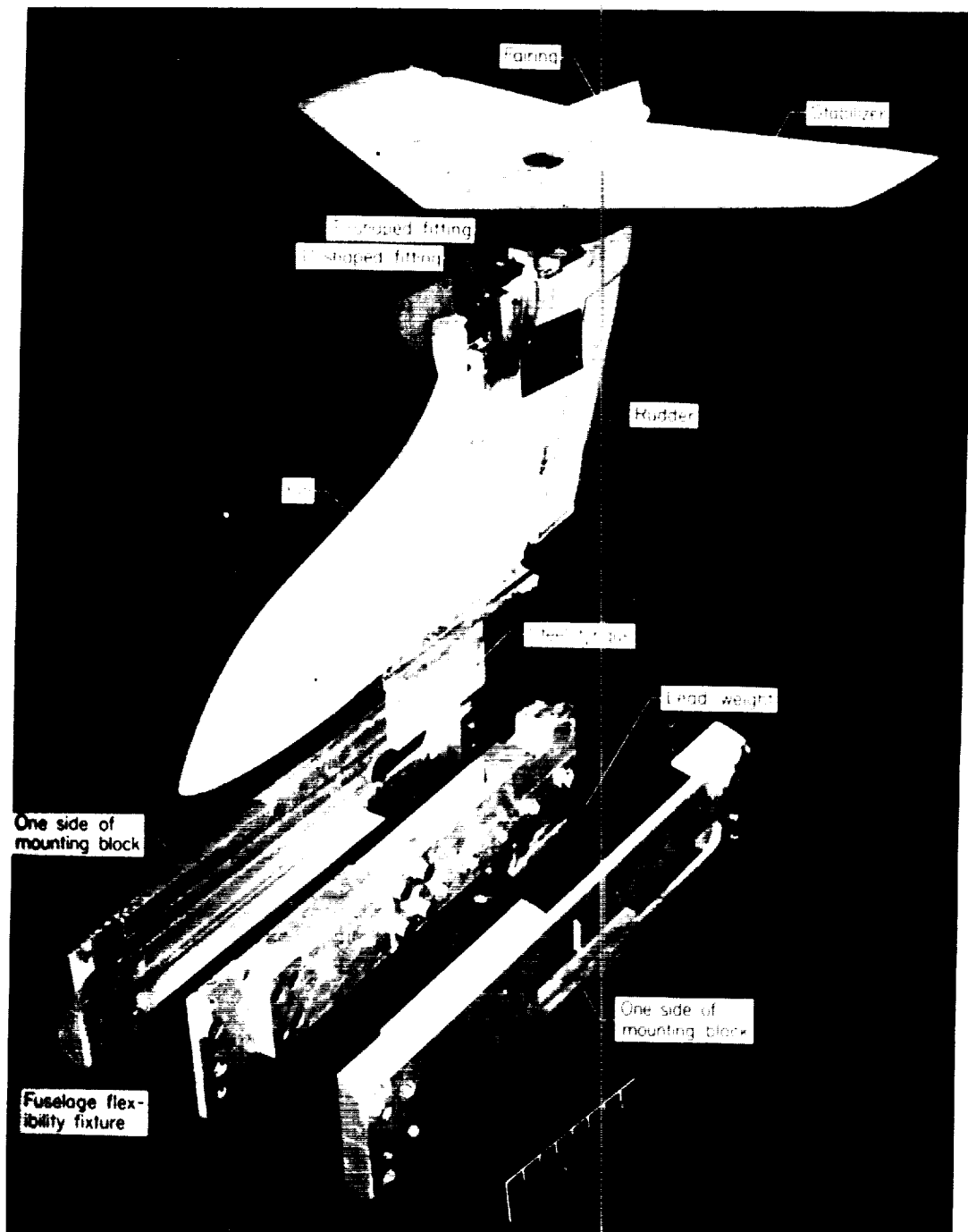
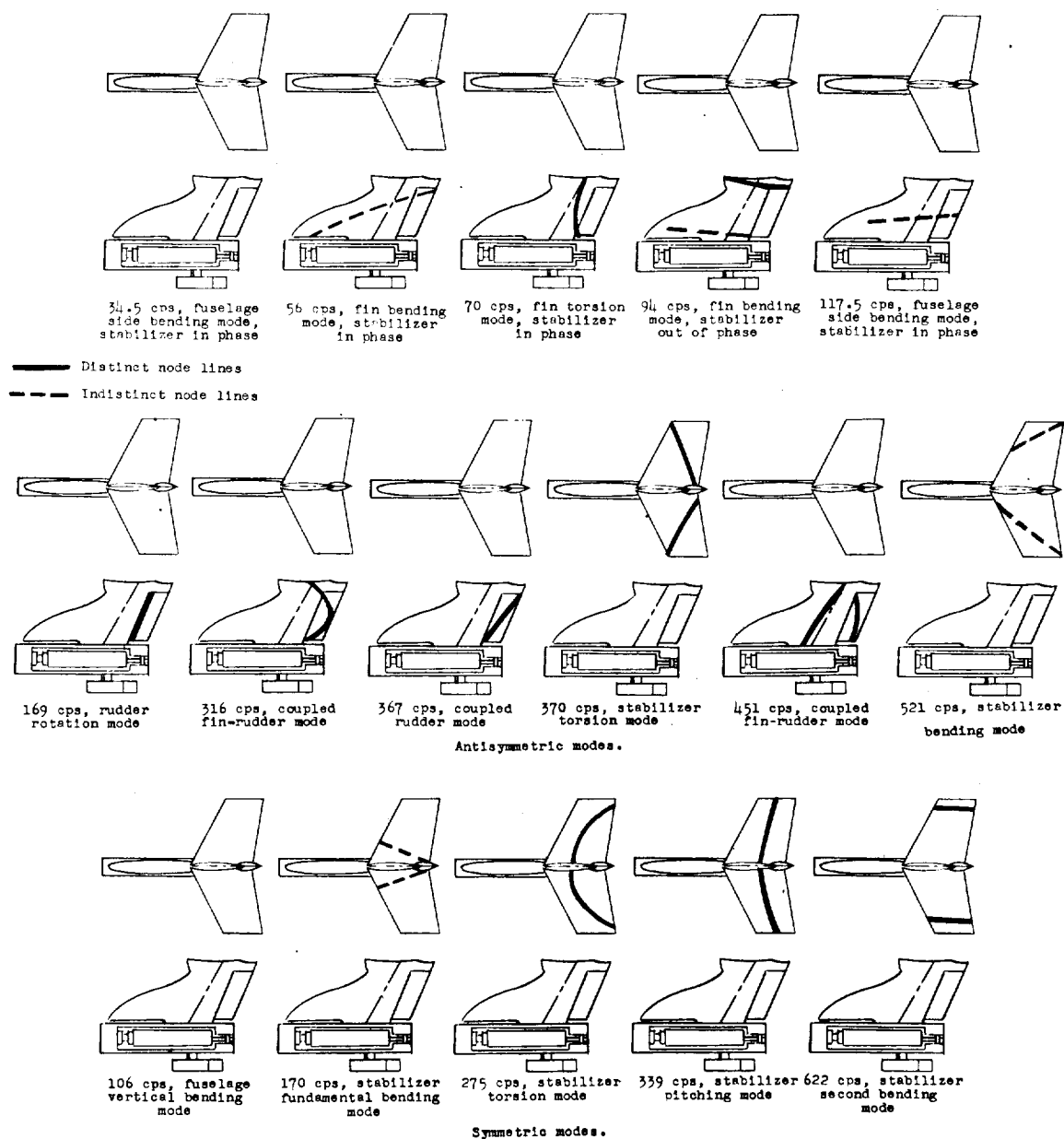


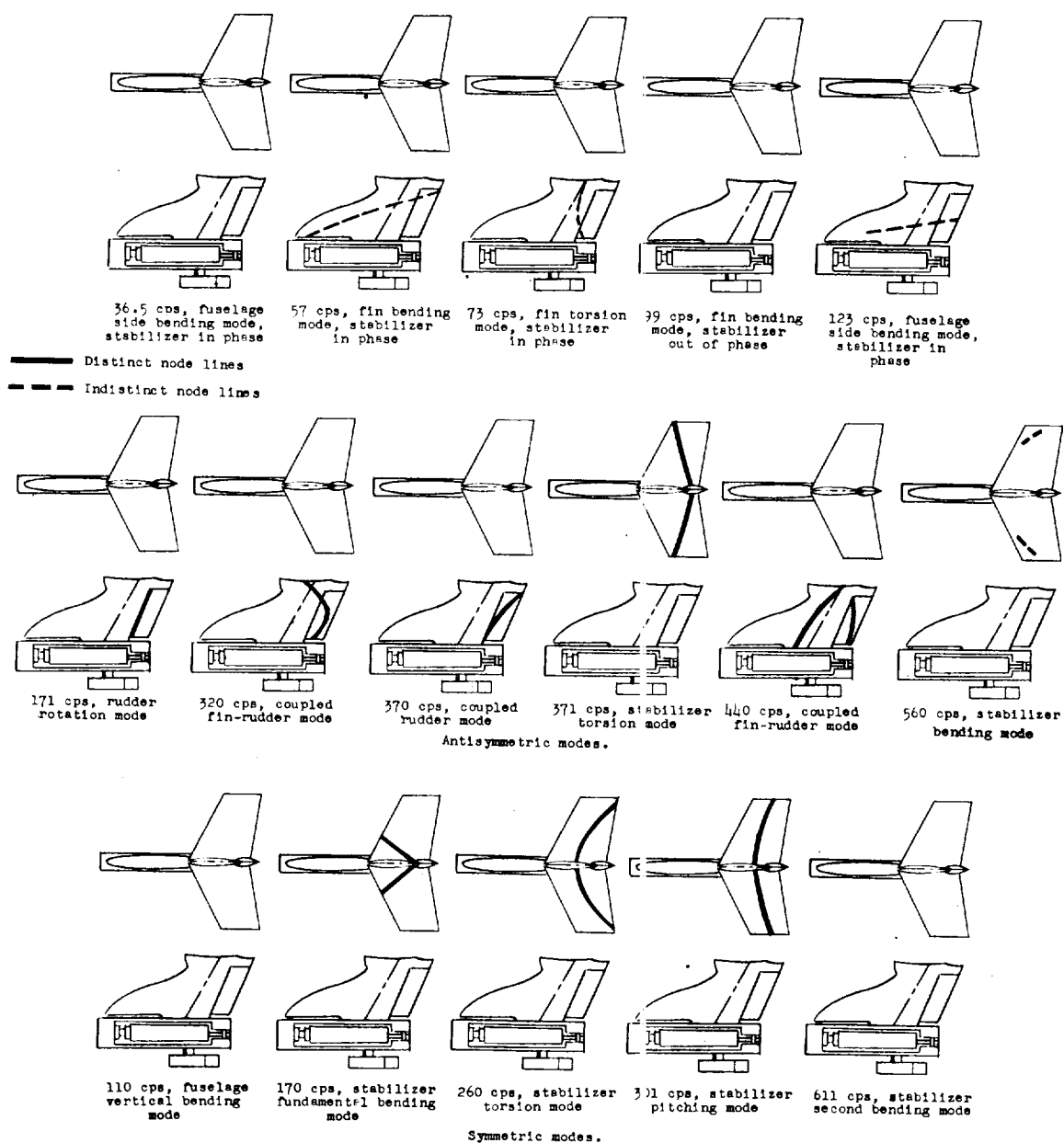
Figure 4.- Exploded-view photograph of model of reference 1 which is similar to models studied in present investigation.

L-57-5190



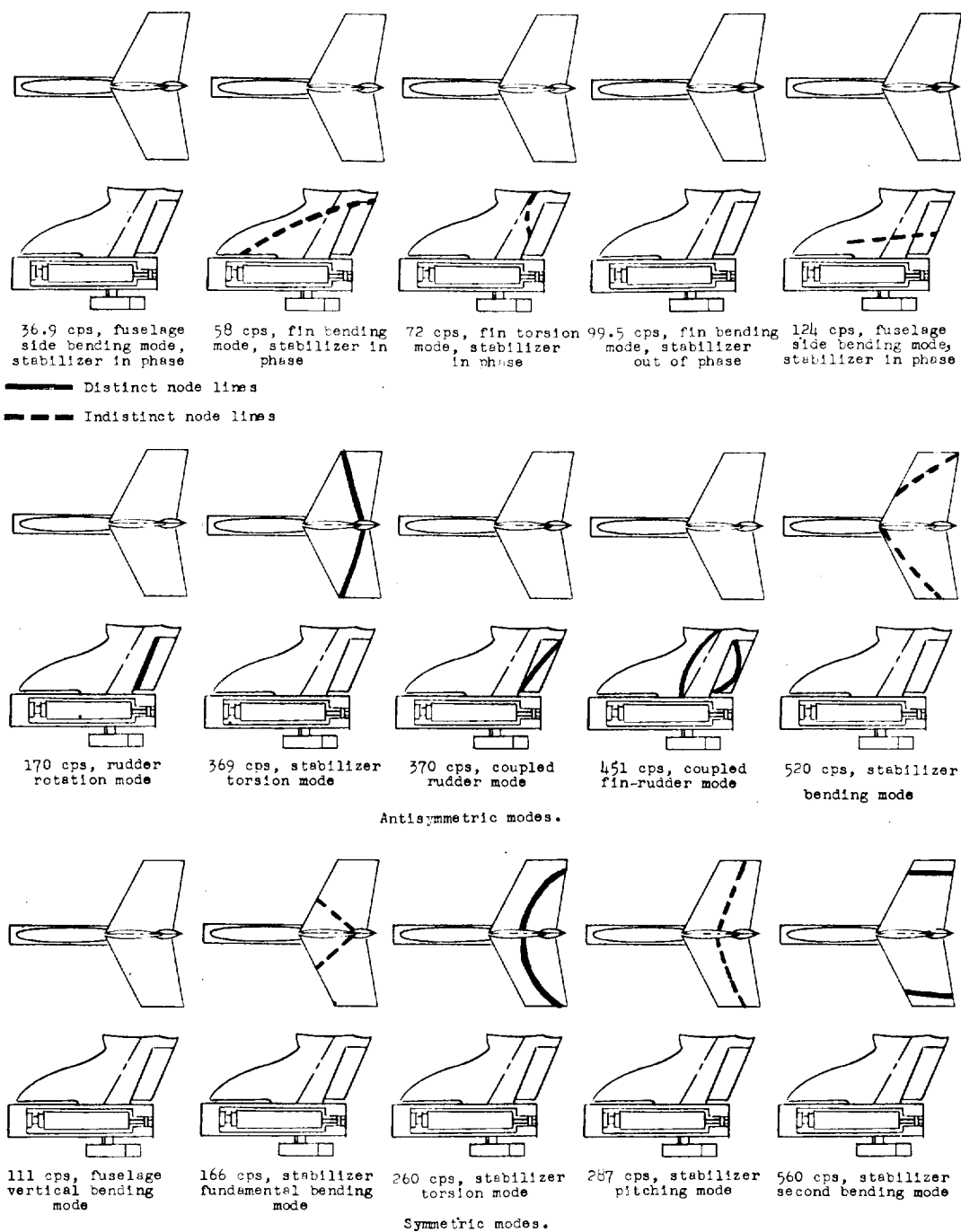
(a) Model 6; normal stabilizer pitch stiffness; runs 2 to 7.

Figure 5.- Node lines and frequencies.



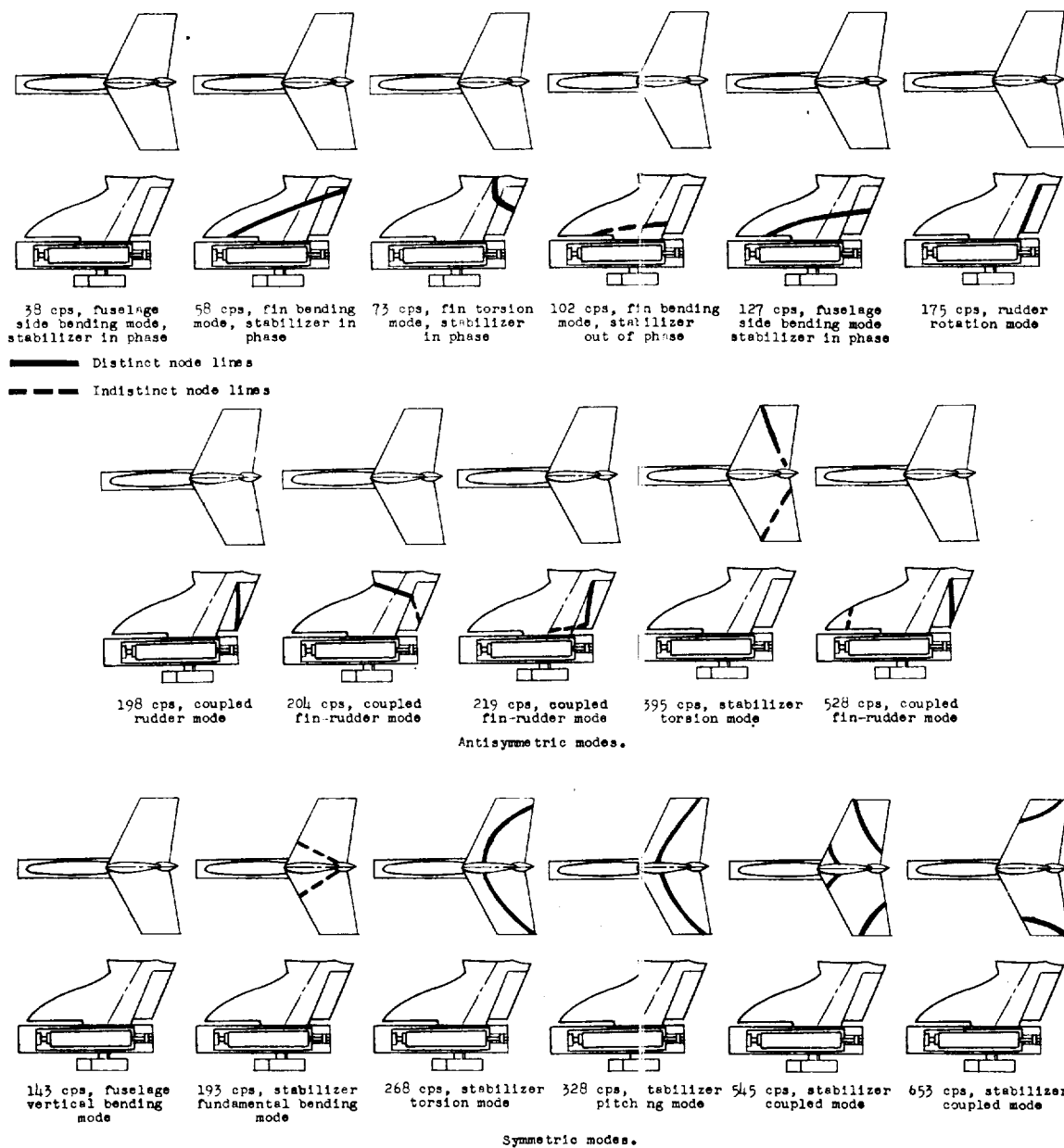
(b) Model 6; emergency stabilizer pitch stiffness; runs 8 to 10.

Figure 5.- Continued.



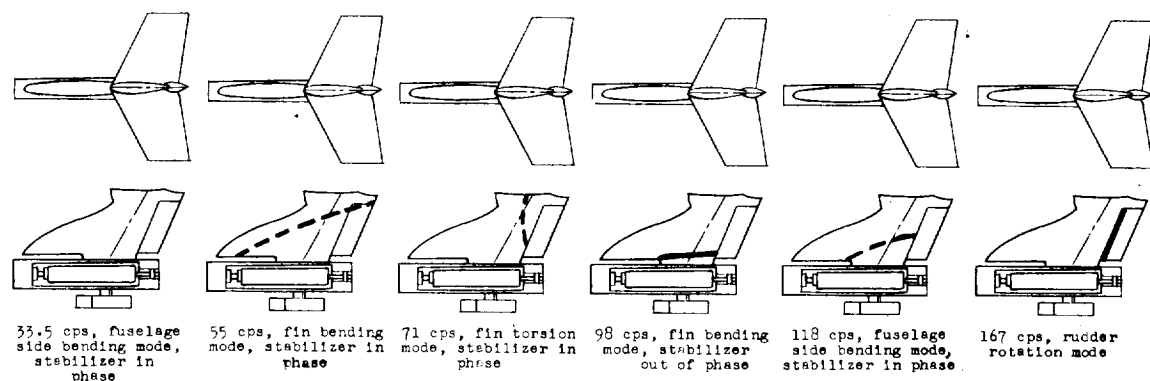
(c) Model 6; emergency stabilizer pitch stiffness; run 11.

Figure 5.- Continued.

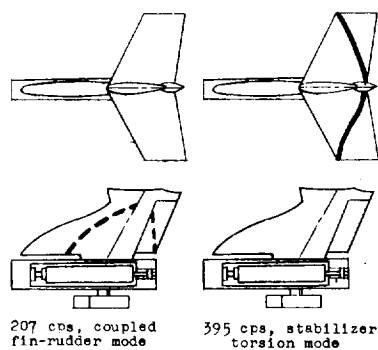


(d) Model 5; normal stabilizer pitch stiffness; runs 13 to 18.

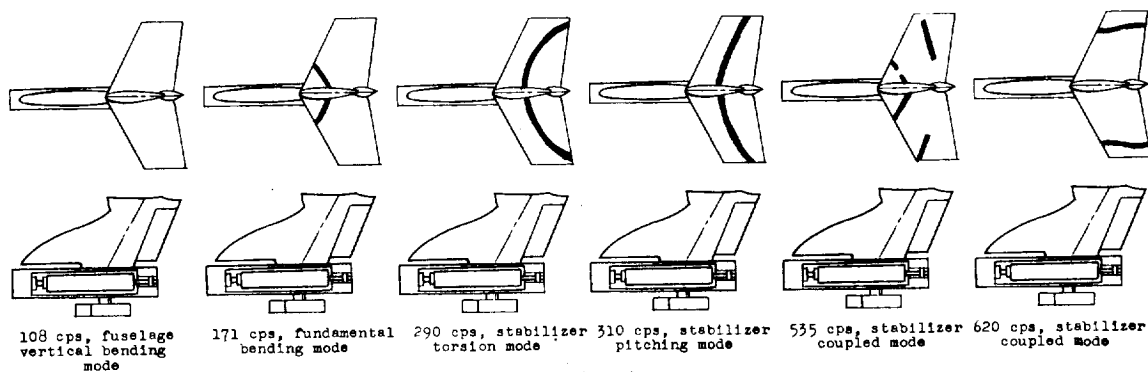
Figure 5.- Continued.



— Distinct node lines
 --- Indistinct node lines



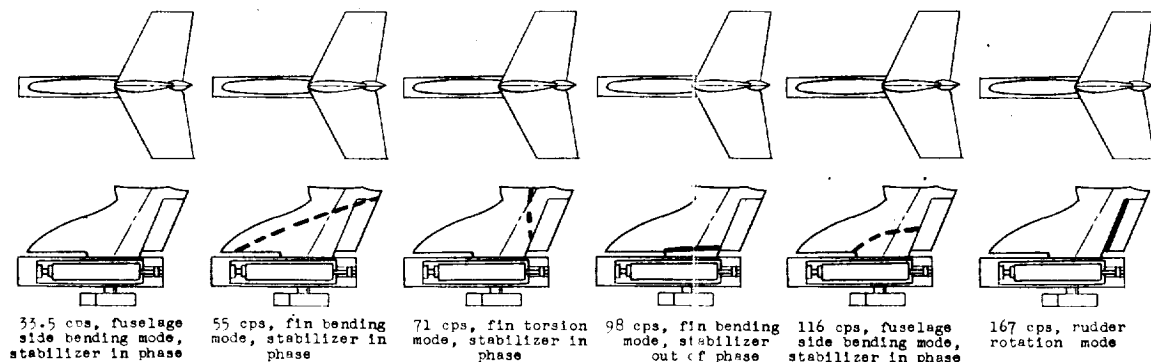
Antisymmetric modes.



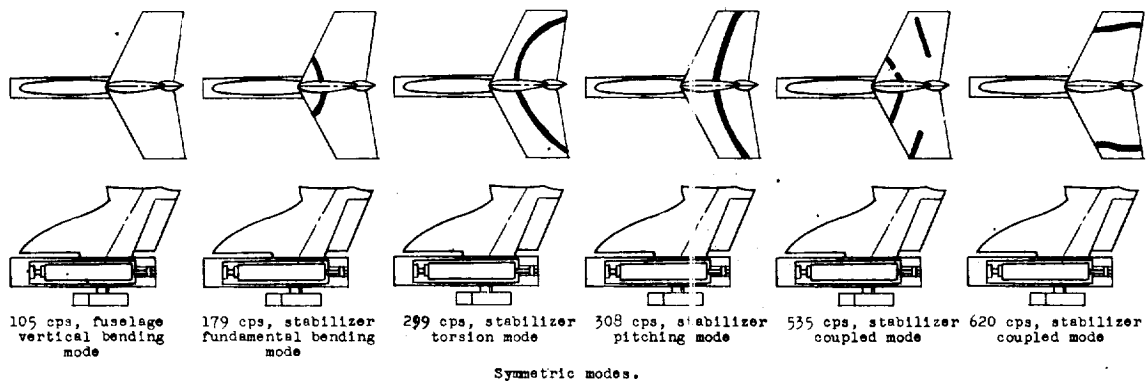
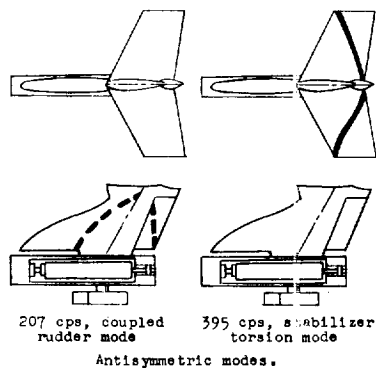
Symmetric modes.

(e) Model 5; emergency stabilizer pitch stiffness; runs 19 to 21.

Figure 5.- Continued.

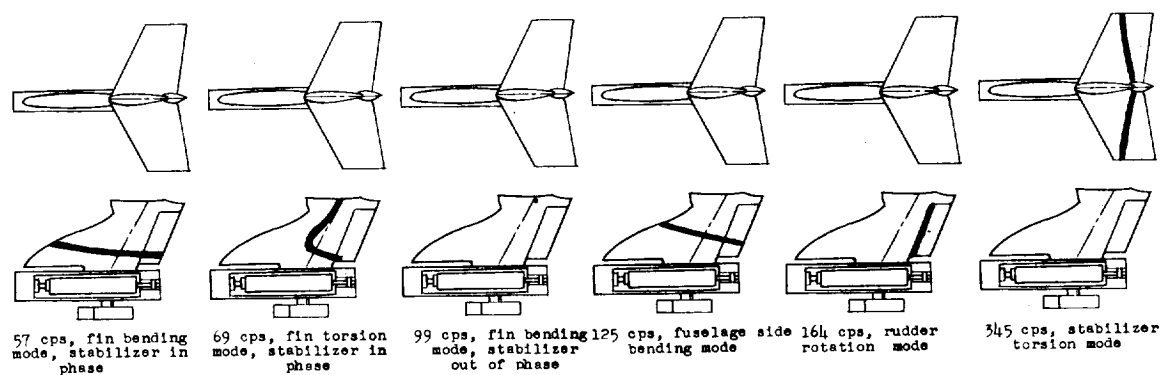


— Distinct node lines
 - - - Indistinct node lines



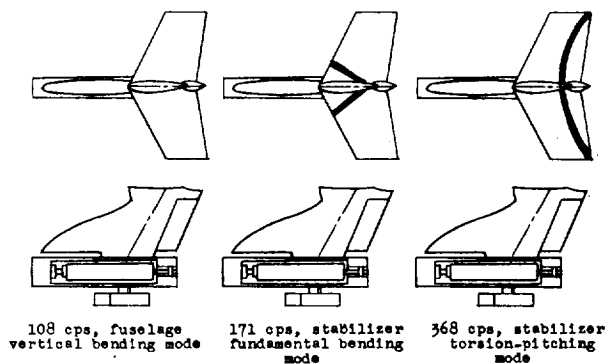
(f) Model 5; emergency stabilizer pitch stiffness; run 22.

Figure 5.- Continued.



— Distinct node lines
 - - - Indistinct node lines

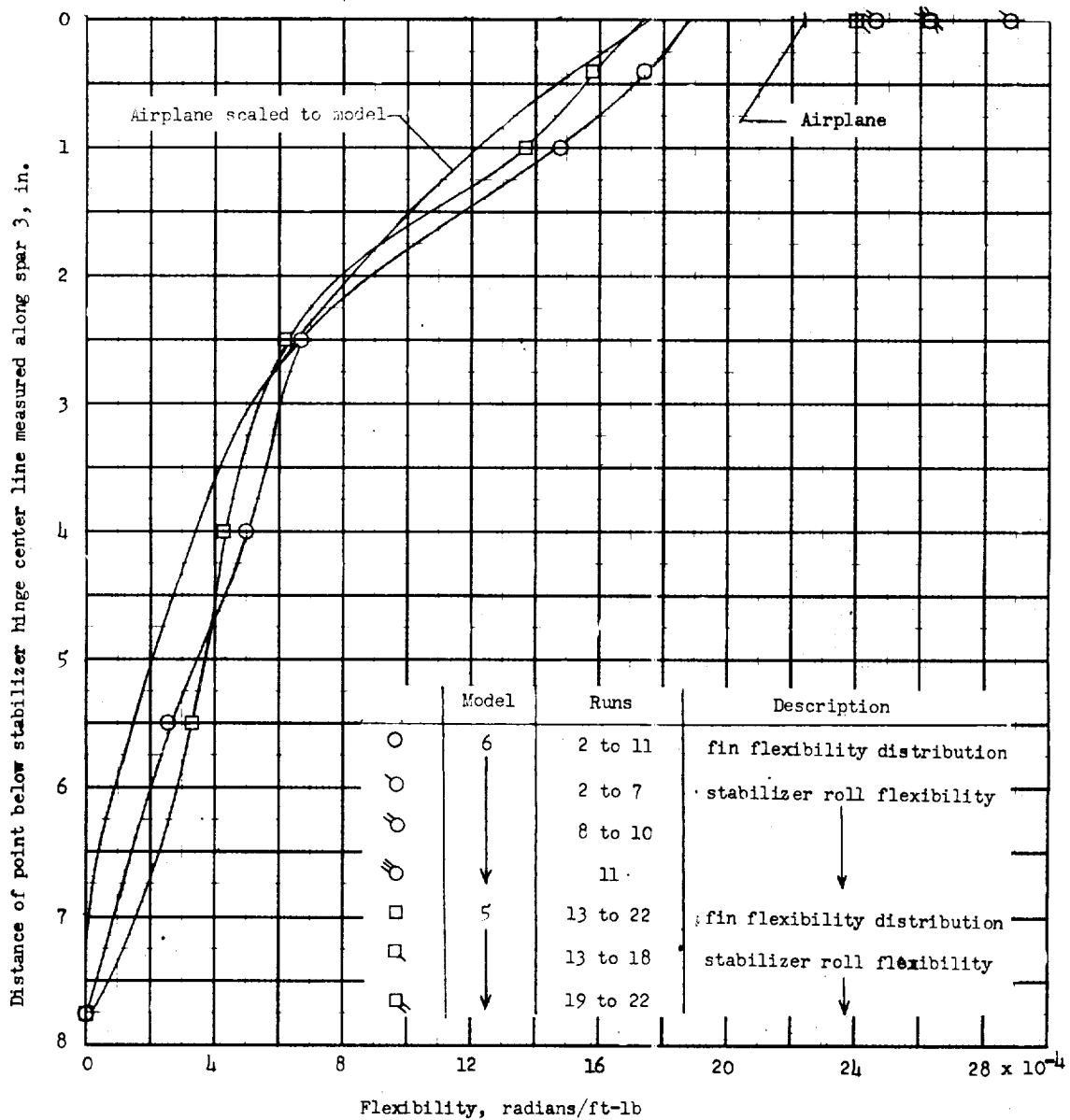
Antisymmetric modes.



Symmetric modes.

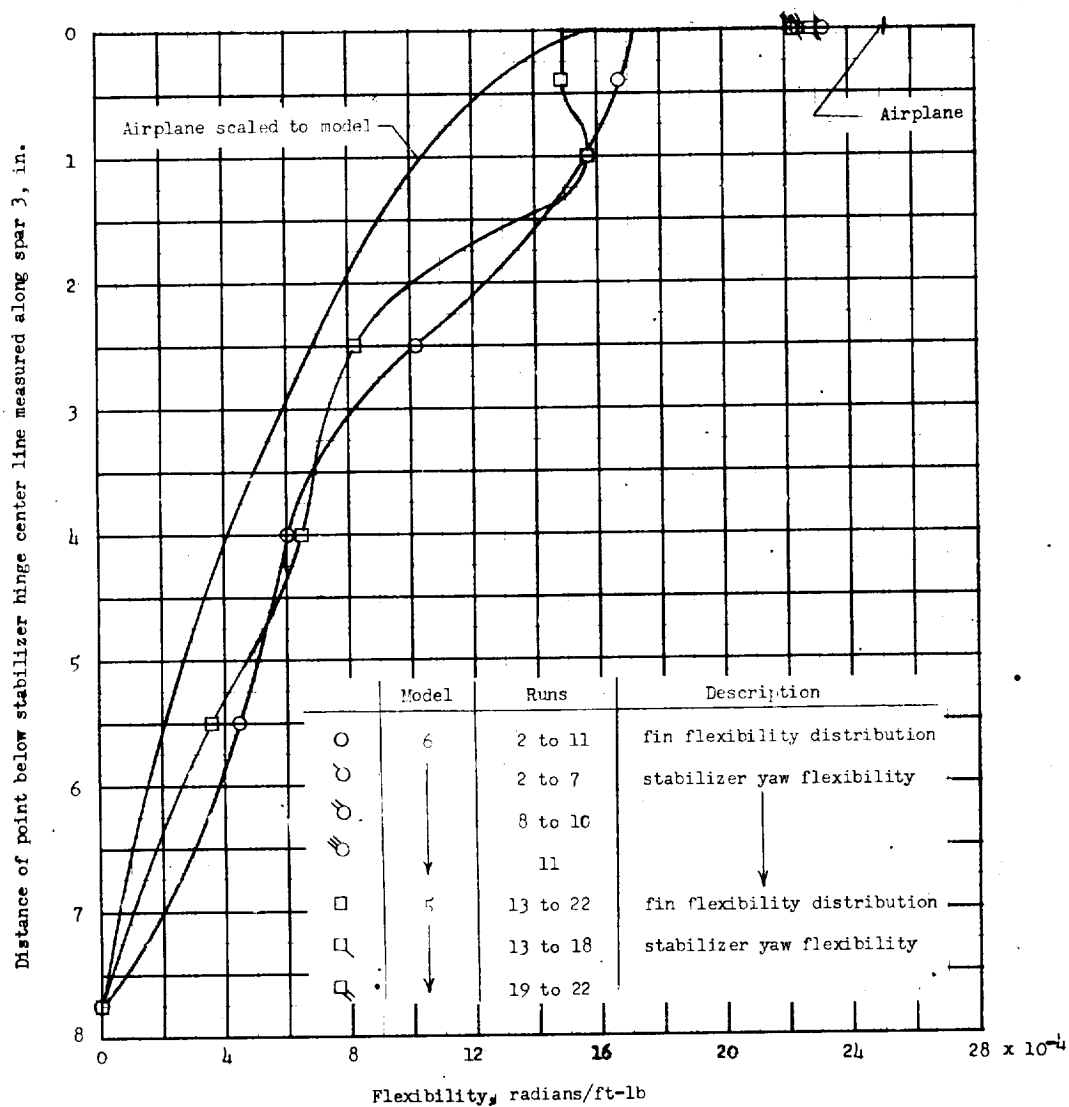
(g) Airplane with normal stabilizer pitching stiffness, scaled to model.

Figure 5.- Concluded.



(a) Fin bending flexibility along spar 3 and roll-roll juncture flexibilities.

Figure 6.- Fin flexibility distribution and fin-stabilizer juncture flexibilities on models.



(b) Fin torsion flexibility about line midway between spar 3 and rear spar, and yaw-yaw juncture flexibility.

Figure 6.- Concluded.

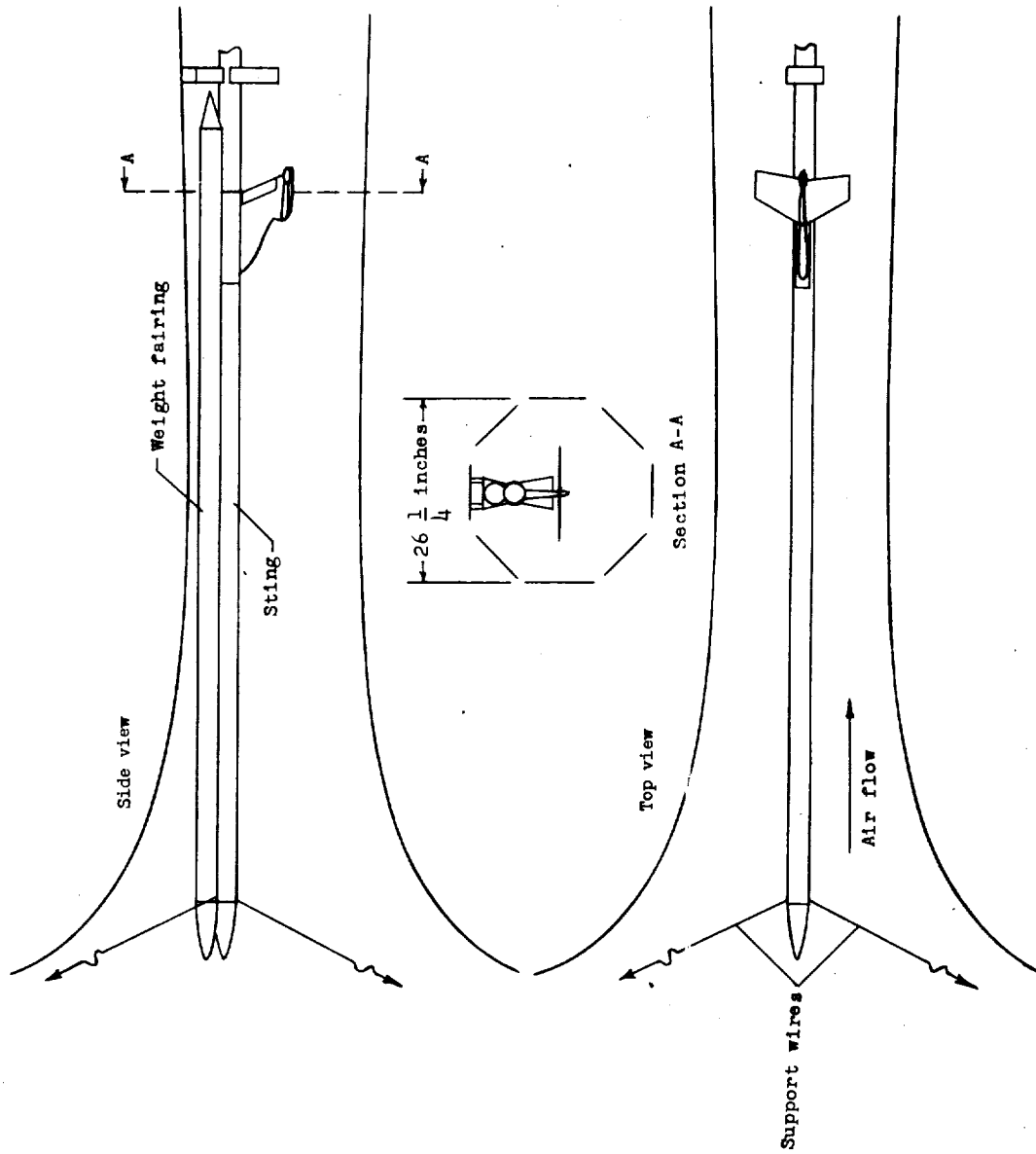
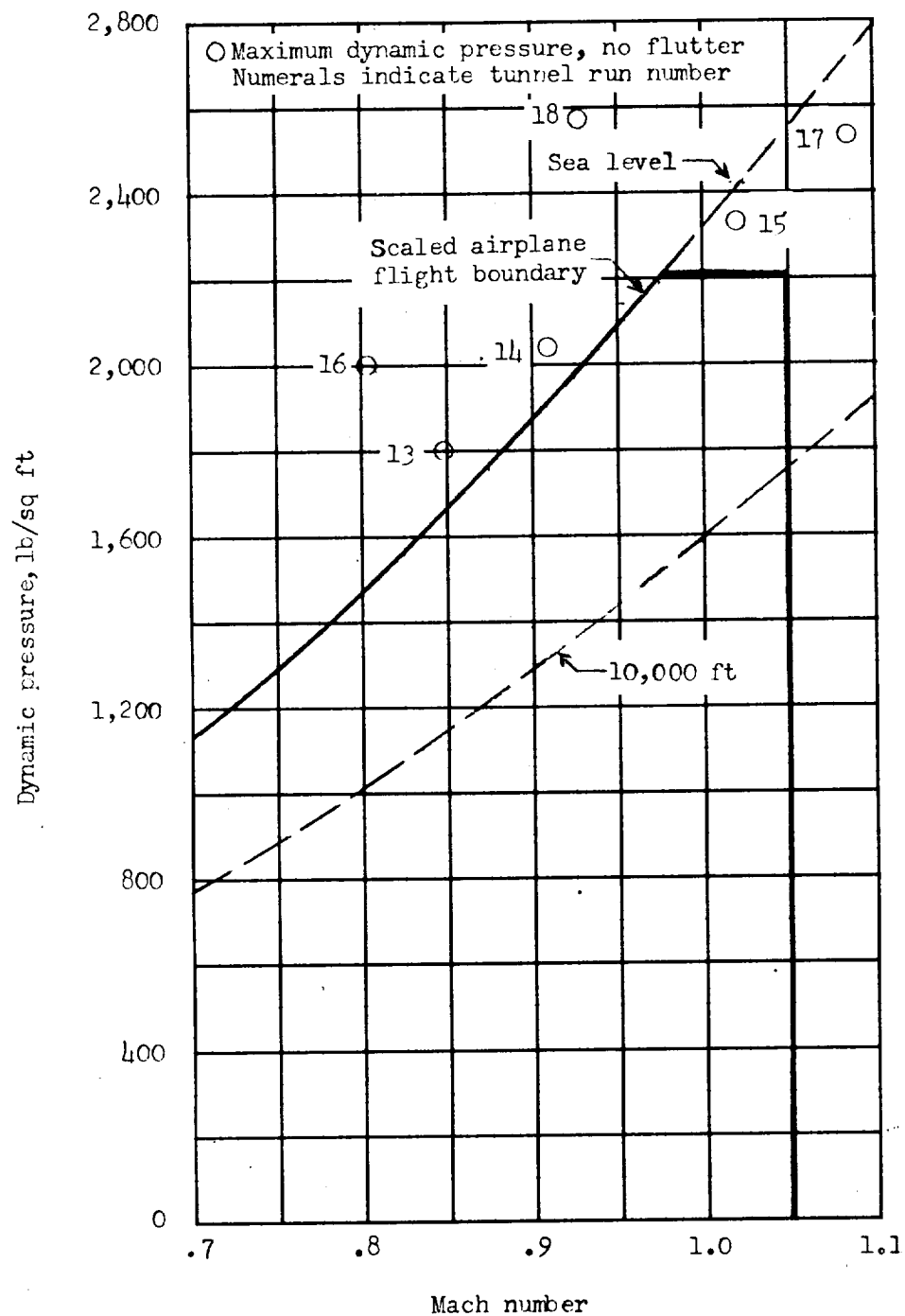
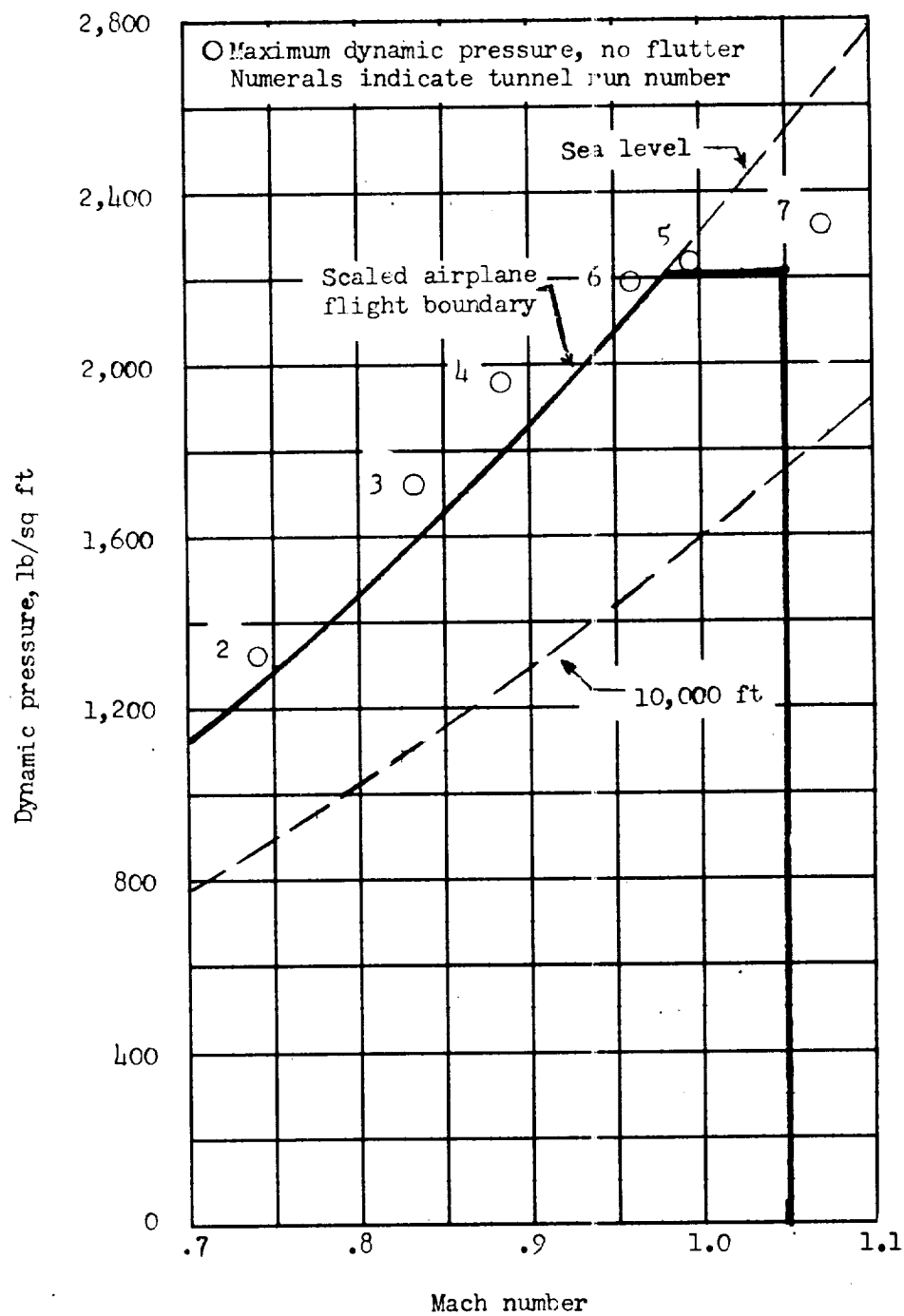


Figure 7.- Sketch of model mounted on sting and installed in tunnel.



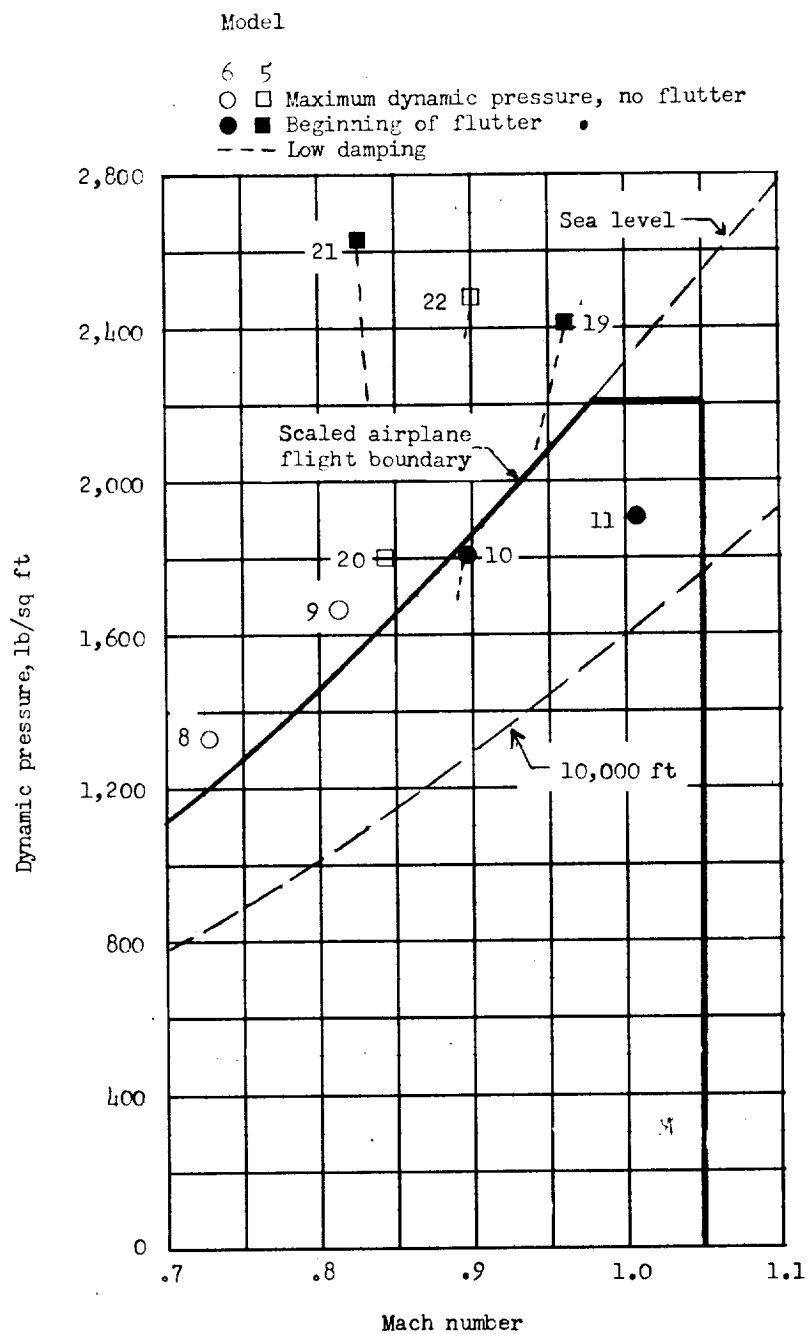
(a) Model 5; antisymmetric model; normal stabilizer pitch stiffness.

Figure 8.- Wind-tunnel test results.



(b) Model 6; symmetric model; normal stabilizer pitch stiffness.

Figure 8.- Continued.



(c) Models 5 and 6; symmetric models; emergency stabilizer pitch stiffness.

Figure 8.- Concluded.

[REDACTED]

.

.

[REDACTED]


NATIONAL AERONAUTICS AND SPACE ADMINISTRATION

TECHNICAL MEMORANDUM SX-242

for the

Office of Naval Research

TRANSONIC FLUTTER INVESTIGATION OF MODELS OF T-TAIL
OF BLACKBURN NA-39 AIRPLANE*




By George W. Jones, Jr., and Moses G. Farmer

ABSTRACT

The models were dynamically and elastically scaled from measured airplane data in accordance with criteria which include a flutter safety margin. The investigation was made in the Langley transonic blowdown tunnel and covered a Mach number range from 0.73 to 1.09 at simulated altitudes extending to below sea level.

INDEX HEADINGS

Airplanes - Specific Types	1.7.1.2
Aeroelasticity	1.9
Vibration and Flutter - Tails	4.2.2



*Title, Unclassified.


[REDACTED]

[REDACTED]

[REDACTED]